Fire Safety Journal 140 (2023) 103869

Contents lists available at ScienceDirect

Fire Safety Journal

journal homepage: www.elsevier.com/locate/firesaf

Fire spread in a large compartment with exposed cross-laminated timber and open ventilation conditions: #FRIC-01 – Exposed ceiling

Andreas Sæter Bøe [a,*], Kathinka Leikanger Friquin [a,b], Daniel Brandon [c], Anne Steen-Hansen [a,d], Ivar S. Ertesvåg [e]

[a] Department of Civil and Environmental Engineering, Faculty of Engineering, NTNU - Norwegian University of Science and Technology, Trondheim, Norway
[b] Department of Architecture, Materials and Structures, SINTEF Community, Trondheim, Norway
[c] RISE Fire Research, Lund, Sweden
[d] RISE Fire Research AS, Trondheim, Norway
[e] Department of Energy and Process Engineering, Faculty of Engineering, NTNU - Norwegian University of Science and Technology, Norway

ARTICLE INFO

Keywords:
CLT
Fire spread
Self-extinction
Large-scale
Compartment fire

ABSTRACT

Exposing cross-laminated timber (CLT) structures in buildings is increasingly popular in modern buildings. However, large timber surfaces, window facades, and different geometries can change the fire dynamics in a compartment. The effect of those parameters, therefore, needs to be studied. Two large-scale CLT compartment fire experiments (95 m^2) have consequently been performed. The experiments were designed to represent a modern office building with an open-plan space and large window openings. In this experiment, #FRIC-01, the ceiling was exposed. The wood crib fire developed slowly and travelled approximately 1.5 m before the ceiling ignited at 32.5 min. Thereafter the fire spread rapidly across the ceiling and wood crib before it shortly after retracted. Three such cycles of rapid spread followed by a retraction occurred within 13 min, whereby the wood crib fire grew larger for each cycle. After the flames extended through the compartment for the fourth time, the fire remained fully developed. After a short period of intense burning, the CLT self-extinguished while the wood crib fire was still burning. The compartment withstood full burnout, and no reignition occurred despite some delamination and using an adhesive that lacks a demonstrated resistance against glue-line integrity failure.

1. Introduction

The use of engineered wood products, e.g., glue-laminated and cross-laminated timber (CLT), has increased massively in recent years. The increased popularity is caused by the many advantages of building with wood, like prefabrication, low carbon footprint, easy handling and mounting, and its aesthetic look. In addition, the implementation of performance-based building regulations and prescriptive regulations with solutions for mid-rise timber buildings have opened the possibility of designing taller timber buildings.

Alongside the development of innovative wood products, there is a potential of introducing new fire risks that previously have not been present. Examples are faster fire spread, larger external flames, and longer fire duration. Over the last decades, several small, medium and large-scale CLT compartment experiments have been performed. These experiments have highlighted several essential features of compartment fires with exposed CLT. One characteristic of these experiments is the increased heat release rate compared to experiments without exposed CLT. This is caused by wood being a combustible material and adds a significant amount of pyrolysis gases to the fire. Also, since most CLT compartment experiments have been ventilation-controlled, a large ratio of the combustible gases has burnt outside the compartment as external flames [1]. This phenomenon has long been known [2,3] and later confirmed by several authors through large-scale experiments [4–7].

However, a recent study [8] has shown that the increase of the external flame with exposed CLT is less for compartments with medium and large openings than previously observed in compartments with small openings. In another study [9], the exposed CLT played a minor role to the size of the external flame when the variable fuel load density was high. Despite increasing the amount of exposed CLT, the external flame size was about unchanged, and only slightly higher temperatures at the facade were measured. This was explained by the high variable fuel load density (1085 MJ/m^2), as the percentage increase of

* Corresponding author.
E-mail address: andreas.s.boe@ntnu.no (A.S. Bøe).

https://doi.org/10.1016/j.firesaf.2023.103869
Received 20 March 2023; Received in revised form 27 June 2023; Accepted 19 July 2023
Available online 24 July 2023

combustible gases from a CLT surface then becomes lower than for a similar compartment with a lower variable fuel load density.

Furthermore, the number of exposed surfaces and their orientation relative to each other affect the fire dynamics and duration [4,10,11]. Another reason for the prolonged fire duration is gypsum board fall-off and delamination of CLT (also known as glue-line integrity failure or premature char fall-off). Both result in fresh wood being exposed to the fire [4,12].

The char layer that forms during combustion of wood gives some protection to the fresh wood behind. To sustain burning, an external heat flux above a critical level must be applied to the surface, otherwise, the burning will stop [13–16]. It is important to note that smouldering may continue for several hours after visible flames are extinguished [17,18]. Smouldering can weaken the structural capacity of timber members [19,20] and transition back to flaming combustion, which eventually might develop into a fully developed fire.

Self-extinction has been observed for compartments with one [12,21] or two [10,22] exposed surfaces. However, the possibility of self-extinction should not be directly connected to the number of exposed surfaces, as it also depends on several other factors, such as the lamella thickness [14,23], the opening factor [24], and the duration of the fire determined by the variable fuel load density.

Although many CLT experiments have been conducted, most have been in relatively small compartments, with openings corresponding to typical ventilation-controlled fires. According to Ref. [25], 70% of all CLT compartment fire experiments had a floor area less than 25 m^2, 86% less than 50 m^2, and 86% had openings corresponding to a ventilation-controlled fire.

With the increased popularity among architects and engineers, CLT is now also found in public and office buildings. These often have large windows to allow for natural light and have open-plan spaces, which is considerably different with regard to opening factor and compartment size compared to most CLT compartment experiments [18,26], but also to compartment fires in general [27].

Overall, due to the size and geometry, buildings with large open-plan areas are often more likely to experience travelling fires. A travelling fire moves in space with a defined leading and trailing edge [28]. Several fire experiments have been conducted to study this phenomenon, like the Edinburgh travelling fire experiments [29], the TRAFIR experiments [30], the X-ONE [31] and X-TWO [32], and the Tisova fire experiment [33]. Fire spread rates in travelling fire experiments in compartments with non-combustible linings have varied significantly. The slowest fires took several hours to travel across the compartment, with flame spread rates of 1–60 mm/min [30,33]. The fastest spread was observed across a 29 m long wood crib in 12 min, with an average spread rate of 2.4 m/min [31].

Travelling fire experiments have predominantly been conducted in compartments with non-combustible surfaces, and the effects of wooden surfaces have barely been studied. Nevertheless, a few recent publications have provided important knowledge to this topic.

A CLT ceiling was found to influence the fire spread rate in a small-scale experiment [34], where the fire spread rapidly across the ceiling once ignition of the ceiling occurred. In the Malveira travelling fire experiment [35], 60% of the ceiling consisted of a combustible cork layer. The fire spread slowly for about 4 h until the fire spread reached below the cork area. From this point on, the fire spread vigorously across the cork ceiling, and the fire front on the wood crib on the floor accelerated quickly. The contribution of the cork was comparable to a wooden ceiling. In the experiments CodeRed #01 [17] and CodeRed #02 [36], the presence of a CLT ceiling caused the fire to spread across the room in 5 and 8 min, respectively. These are the largest compartment fire experiments with exposed CLT performed to date, with a floor area of 352 m^2. The flames impinged at the CLT ceiling shortly after ignition of the wood crib on the floor and caused ignition of the ceiling within 3 min in CodeRed #01 and 5 min in CodeRed #02. The flames spread quickly across the ceiling and reached the end of the compartment approximately 2.5–3 min later, corresponding to an average spread rate of approximately 9 m/min. In CodeRed #01, the leading edge of the ceiling flames reached the end of the compartment 20 s before the leading edge of the wood crib, which demonstrates that the radiation to the floor was intense. The impact of the CLT ceiling was clearly demonstrated, as the results could be directly compared to the identical experiments without exposed CLT, X-ONE [31] and X-TWO [32]. In these experiments, the fire spread across the room in 12 and 22 min, respectively. In addition to the increased fire spread rate, the heat release rate was doubled, and external flames were visually larger.

The few travelling fire experiments with a combustible ceiling have revealed that the current understanding of fire dynamics and fire spread in large open-plan compartments with exposed CLT is limited. The flame spread rates in the experiments with a combustible ceiling significantly exceeded the flame spread rates found in compartment experiments without exposed combustible surfaces ($\leq$1 m/min) [37–41]. Such fast fire spread rates might impact available evacuation time, and the fire size can be significant before the fire brigade arrives [42].

These findings suggest that it is essential to expand the knowledge on how exposed CLT affects the fire spread and fire safety in large open-plan spaces with CLT [25,43,44]. This includes a better understanding of the feedback mechanisms between the combustible surfaces and the variable fuel load and how this interaction changes the fire dynamics, fire spread, fire duration and external flames. Due to the low number of large open-plan compartment experiments with exposed CLT, many aspects are not yet studied at full scale. The experiments performed to date have:

- comprised compartments with relatively small openings, which allowed significant collection of the smoke layer under the ceiling before ignition,
- involved impingement of the initial fire on the ceiling, which might in practice not occur for compartments with high ceilings and smaller ignited items,
- not involved exposed wall surfaces.

To increase the knowledge of fire development and fire dynamics in well-ventilated, large open-plan compartments with exposed CLT, and address the points listed above, two large-scale experiments have been conducted. The aim was to study the fire development and spread, heat release rate, temperature distribution inside the compartment, charring rate for the CLT, and external flames, for different configurations of exposed CLT surfaces. The first experiment, #FRIC-01, had exposed CLT in the ceiling, while in the second experiment, #FRIC-02, the ceiling and one wall were exposed. The first experiment is described and analysed in this article.

2. Methods

2.1. Methodology

The experiment was designed to study how exposed CLT, large ventilation openings and a large open-plan area affect the fire development and spread in a compartment. The fire development, flame heights and flame spread are studied through visual observations, measured temperatures in the compartment and heat flux towards surfaces, and calculations of the heat release rates for the variable fuel and CLT.

2.2. Experimental setup

2.2.1. Compartment

The compartment in the experiment was built of CLT elements in three walls and the ceiling, while the fourth wall was almost entirely open with four large openings. The CLT elements in the roof rested on the three CLT walls. They were supported on the fourth wall by a 140

mm × 315 mm glulam beam resting into a pre-cut hole in the CLT end walls and supported by three aerated concrete columns. The inner geometry of the compartment was 18.80 m × 5.00 m x 2.52 m (L x W x H). Deviations up to ±0.05 m were present for the ceiling height caused by a slightly tilted floor, with the highest level by the window wall. The deviations are not included in the drawings. A sketch of the experimental setup is shown in Fig. 1, and pictures of the compartment are given in Figs. 2 and 3.

The beam and the three columns in the window wall created four openings of 4.25 m width and 2.20 m height, with a total opening area of 37.4 m^2. This corresponds to an opening factor (OF) of 0.18 $m^{1/2}$ calculated by $OF = A_V.H_V^{1/2}/A_T$, where A_V and H_V represent the area and height of the openings, while A_T is defined as the total area of the enclosure surfaces, including the opening areas [45].

The roof consisted of eight CLT elements overlapping with a lap joint, while the back wall was built of four elements. The roof elements were 5.14 m long and 2.45 m wide, while the back wall elements were 2.45 m tall and 4.82 m wide. The CLT elements in the back wall and ceiling were 140 mm thick and made of 5 layers (40-20-20-20-40 mm), while the end walls were built of 80 mm thick CLT with three layers (30-20-30 mm). The CLT elements were produced in accordance with EAD 130005-00-0304 [46]. The wood in the elements was Norwegian spruce, and the glue between the layers was a regular polyurethane adhesive named Loctite 2 HB-S. The density of the CLT elements was approximately 484 kg/m^3 (based on measurement of one element), with moisture content (dry value) of 12.8% ± 0.3% (standard deviation, n = 48) measured with a moisture meter. The exposed CLT area was 95% (89.3 m^2) of the floor area since the glulam beam and some insulation covered approx. 0.25 m of the ceiling width, see Fig. 3 and further details below.

Two façade walls were positioned above Windows 2 and 4 to provide a more realistic behaviour of the external flame. The façade walls were 2.45 m high and 5.00 m wide. They were built up by a wooden frame covered by a 12 mm thick oriented strand board and 30 mm thick stone wool insulation on the exposed side, see Figs. 1 and 2.

The compartment was built on a concrete floor, which was protected by 30 mm thick stone wool insulation to prevent concrete spalling during the experiments. The walls were protected by two layers of 15 mm thick fire-rated gypsum boards Type F [47]. The outer gypsum board layer was shifted with a half board width to the innermost layer to avoid continuous joints leading directly into the wood. Both layers were fastened by 41 mm long gypsum board screws. The screws were positioned 50–70 mm from the board edge and with 350–400 mm distance between screws. A screw pattern template was used to ensure a similar screw pattern for all gypsum boards.

The glulam beam and edges of the CLT at the front wall were protected with two layers of 25 mm thick ceramic fibre insulation. The outer layer was shifted half a width to avoid overlapping joints. The outer layer covered 100 mm of the exposed CLT ceiling along the glulam beam.

The experiment was performed outdoors. On the day of the experiment, the weather was cloudy, with negligible wind and no precipitation. The temperature at the start of the experiment was 15 °C and gradually increased to 20 °C during the experiment.

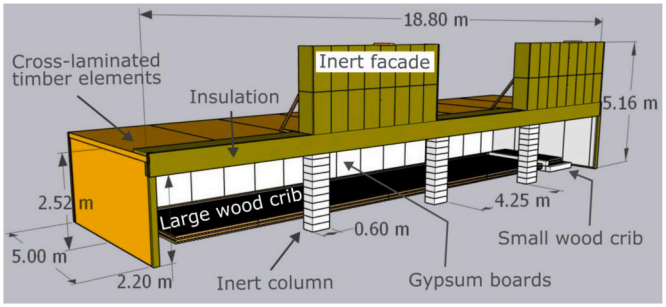

Fig. 1. Sketch of the compartment.

Fig. 2. The compartment with the burning wood crib fire before the ceiling was ignited. The small crib is at the right end of the compartment. The fire shows at which end the wood crib was ignited.

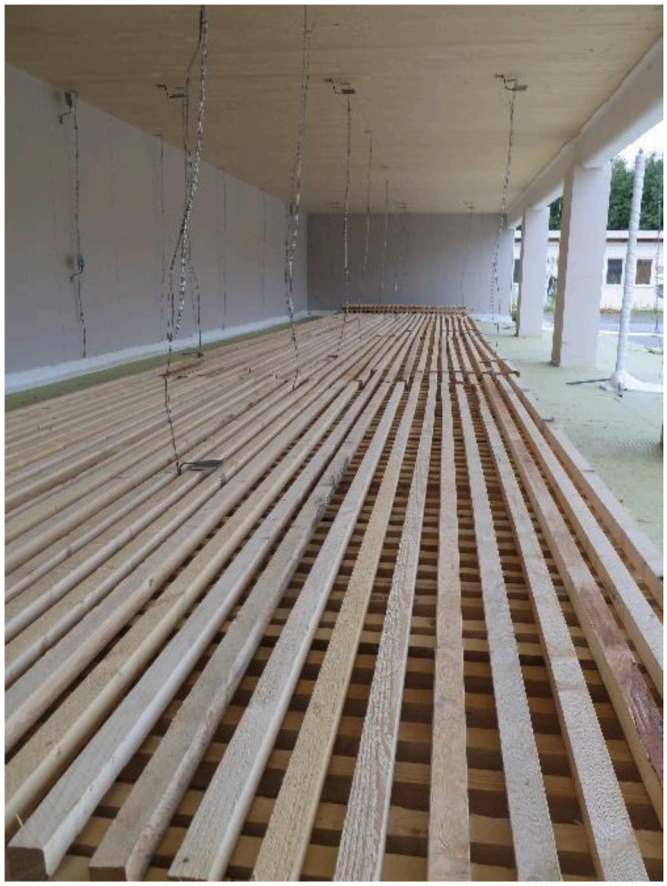

Fig. 3. View from inside the compartment, showing the large wood crib, the exposed CLT ceiling and the protected walls. The glulam beam (above window openings) is covered with ceramic fibre insulation, creating a reservoir height of 0.36 m.

2.2.2. *Wood crib*

The variable fuel load in the compartment was represented by a long continuous wood crib, 15.5 m × 2.8 m x 0.2 m, and a smaller wood crib, 1.0 m × 2.8 m x 0.2 m. The small crib was placed on a scale 0.2 m higher than the large crib. The large and the small cribs are hereafter referred to as one unit, "the wood crib". The wood crib contained wood sticks with a cross-section of 50 mm × 50 mm, stacked horizontally on top of each other in four layers, where the sticks in each layer were perpendicular to the previous layer. The sticks laid perpendicular to the crib length were 2.8 m, while the parallel ones were 4.3 m long. The moisture content was measured by drying samples of the sticks in an oven, according to ISO 12570 [48]. The average moisture content was 14.5%, with 13% ±

0.8% (standard deviation, n = 20) and 16% ± 0.6% (standard deviation, n = 20) for the short and long sticks, respectively. The difference in moisture content between the long and short sticks was likely caused by different storage conditions during the two last weeks before the experiment. The wood used was Norwegian spruce, with an average density of 486 kg/m^3 ± 40 kg/m^3 (standard deviation, n = 25). The distance between the sticks was 50 mm, which gave a crib porosity factor of 0.19 cm. The porosity factor is related to the ratio of the mass flow rate of air to fuel inside vertical shafts of a crib, expressed through dimensions of the crib [49]. 0.19 cm corresponds to the open regime, where the crib burning is not controlled by the porosity (spacing between the sticks) but rather by the thermal feedback from the compartment and the geometry of the wood crib [49]. The total mass of the crib was 2065 kg, determined by weighing all sticks. This corresponds to a fuel load density of 353 MJ/m^2 (per floor area) when using a heat of combustion of 16.0 MJ/kg (see Section 2.4.2 for derivation).

2.2.3. Ignition

Ten aluminium metal trays with dimensions 150 mm × 220 mm × 50 mm (L × W × H) were positioned at 70 mm distance to each other directly below the edge of the wood crib at the left end of the compartment to get a uniform fire across the width of the crib. The first stick of the bottom wood crib layer was removed to make room for the trays to be positioned with 1/3 of the tray directly below the crib. Each tray was filled with 0.5 L of heptane, with a total amount of 5.0 L.

2.3. Instrumentation and measurements

Temperature and incident radiant heat flux at different locations inside the compartment were measured with 120 thermocouples (TC) of type K 1.5 mm [50] and 24 plate thermometers (PT) [51]. TCs are commonly used to measure gas temperatures, although they are slightly affected by radiative heat transfer. The PTs measure surface temperatures of materials with good insulation properties and may be used to calculate the adiabatic surface temperature and the incident radiative heat flux towards the surface [52] (see Section 2.4.1).

Positioning of the TCs was chosen to measure temperature distributions in X, Y and Z-direction at strategic locations. The zero-point for X, Y and Z was defined on the floor at the inner side of the left end wall in the window opening. The thermocouples were arranged in TC-trees, where the TCs were attached to a steel chain (Ø4 mm) hanging from the ceiling. Due to the varying ceiling height of ±0.05 m, the TCs were aligned with reference to the ceiling. For easier reading throughout the article, the TC height from the floor is presented as if the ceiling height was constant at 2.52 m. A detailed overview of the positions of all sensors is given in Figs. 4–6.

TCs and PTs were mounted on the façade above Windows 2 and 4 to estimate the incident radiant heat flux from the external flame, see

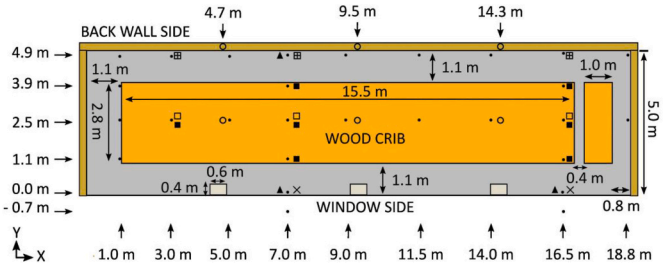

Fig. 5. Instrumentation in the XY-plane (plan view). For symbols, see Fig. 4.

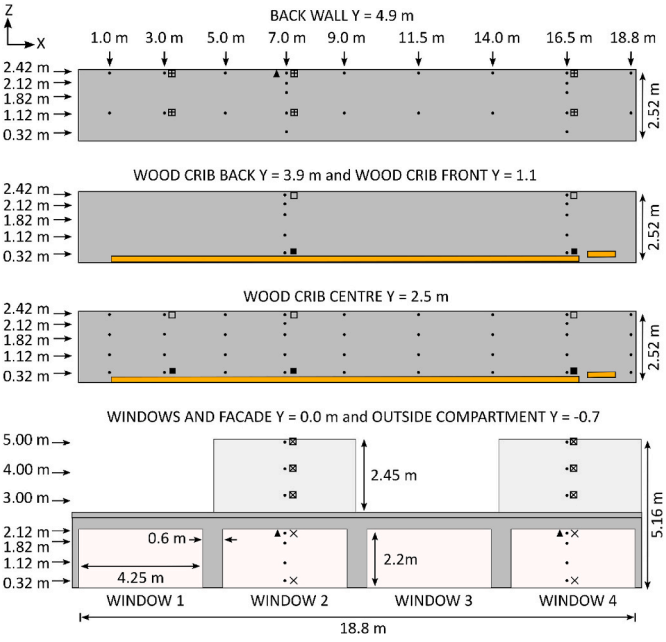

Fig. 6. Instrumentation in XZ-plane. For Y = −0.7 m, only TCs are present, no gas sensors or bidirectional probes. For symbols, see Fig. 4.

Section 2.4.1. The PTs were flush with the insulation surface, while the TCs were located next to the PTs 20 mm in front of the façade. The TCs and PTs were positioned 0.8 m, 1.8 m, and 2.8 m above the top of the window opening. A TC-tree was located 0.7 m in front of the façade walls to measure the flame temperatures. The distance of 0.7 m was chosen based on this being the centre of the flame according to the Law-model [53], where the depth of the external flame is equal to 1/3 of the window height. Two PTs were located 8.0 m in front of the compartment. However, due to an unknown error, these gave no signals during

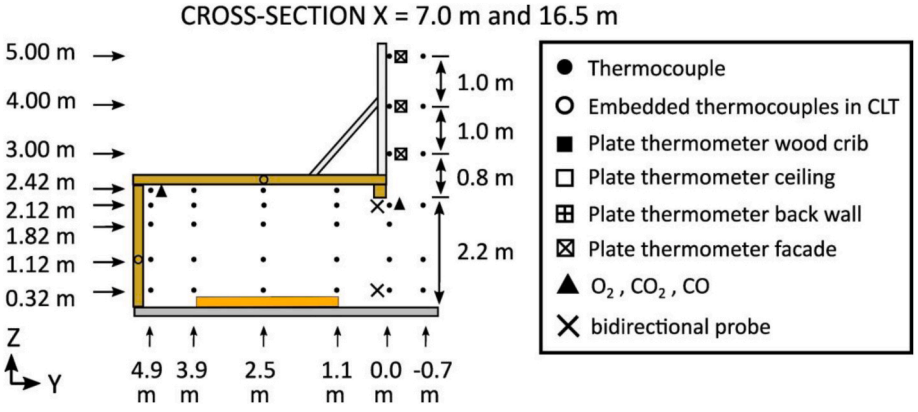

Fig. 4. Instrumentation in the YZ-plane (cross-section) at X = 7.0 m and 16.5 m. For X = 16.5, only gas measurements in the window opening.

the experiment.

The experiment was recorded by eight video cameras, including three IP cameras at a 15–20 m distance, an air-cooled GoPro camera, a water-cooled 360° camera inspired by Hoehler [54], two water-cooled GoPro cameras in Pyrex columns with circulating water, and a drone. Video recordings were used to evaluate fire spread and flame heights.

Gases were sampled from the compartment at three different locations, see Figs. 4–6. The gas was cooled and dried before the oxygen (O_2), carbon monoxide (CO) and carbon dioxide (CO_2) concentrations were measured by a gas analyser. The measurement ranges for the different gas sensors were 0–21% for O_2, 0–10% for CO_2 and 0–5000 ppm for CO. Four bidirectional probes [55] were used to measure the gas velocity in and out of Windows 2 and 4, as shown in Figs. 4–6.

To monitor the temperature development in the CLT, 1.5 mm sheathed TCs type K were embedded into some elements at 0, 10, 20, 30 and 40 mm depth from the element surface at locations: X = 4.7, 9.5 and 14.3 m. The TCs embedded in the back wall were installed at 1.12 m height, and the TCs embedded in the ceiling were installed at the centre line of the room, Y = 2.5 m. The TCs were installed in 1.6 mm holes drilled 40 mm into the elements from the rebate joint parallel to the isotherm, as this was considered the most reliable method for measuring the temperature [56–58]. The holes were drilled with a drill guide to get perpendicular holes and in a zig-zag pattern to increase the vertical distance between overlaying holes, see Fig. 7. The TC wires were embedded into the wood through pre-cut slits to protect the wire from mechanical damage during construction, and to not cause an air gap in the joint after installation. The embedded TCs of the back wall were used to measure the temperature behind the gypsum boards and inside the CLT. Due to a logger error, data were only available from the embedded TCs at X = 14.3 m.

The temperatures of the embedded TCs were also used to calculate the charring rates at different depths into the CLT. The charring rates were calculated from the time difference of two embedded TCs to reach 300 °C. The 300 °C isotherm is considered the location of the charring front [59].

After the experiment, the char depth was measured on five of the eight CLT elements in the ceiling with a method inspired by Ref. [60]. A 500 mm × 500 mm grid pattern was drawn on the unexposed side of the CLT, and perpendicular holes were drilled in each cross-point. The char layer was then physically removed by a steel brush around each drilled hole, and the remaining thickness of the CLT was measured by a digital calliper. The total thickness of the CLT had increased by 2 mm due to increased moisture content caused by the manual suppression of the fire with water. This increase was corrected for in the calculation of the char depth, as the increase, in general, could be assigned to the four intact layers.

2.4. Data analysis methods

2.4.1. Method to determine incident heat flux

Measurements from the PTs and TCs were used to determine the incident radiation heat flux [W/m^2] through equation: $\dot{q}''_{inc} = \sigma T_{PT}^4 + (1/\varepsilon)[(h+K)(T_{PT}-T_g)+C(T_{PT}^{j+1}-T_{PT}^{j})/\Delta t]$ [52], where ε is the emissivity of the PT (0.9), σ is the Stefan-Boltzman constant ($5.67 \cdot 10^{-8}$ W/(m^2 K^4)), T_{PT} is the temperature of the PT, T_g is the gas temperature, h is the convective heat transfer coefficient (10 W/m^{2}K), K is the thermal conduction coefficient (8 W/(m^{2}K)), and C is the heat capacity of the PT (4200 J/(m^{2}K)). j and j+1 represent two consecutive data recordings, and Δt is the corresponding time difference. Here, Δt was 1 s. The gas temperature was approximated using the 1.5 mm TC close to the PT. It is noted that this measurement is influenced by radiation. However, the error of this approximation has a negligible influence on the upper range of incident radiant heat fluxes measured.

2.4.2. Heat release rate of the wood crib and CLT

The method to estimate the heat release rate (HRR) for the wood crib was inspired by the method used in X-ONE [31]. It was also used in the CodeRed experiments [17] and consists of three steps: 1) Determine the mass loss rate (MLR) per unit length of the wood crib. 2) Integrate over wood crib length to find the total MLR. 3) Convert MLR to HRR.

In contrast to the method of [31], the MLR per unit length in this experiment was based on a real MLR measurement from the small wood crib (1.0 m × 2.8 m) positioned on a scale at the right end of the compartment, see Fig. 1. This is considered an improvement as the MLR changes with time and is not a constant value through the duration of the fire. The HRR was approximated by $\dot{Q} = \dot{m}\,\Delta H_C\,\chi$, where the mass loss rate ($\dot{m}$) is multiplied by the net heat of combustion (ΔH_C) and a combustion efficiency factor (χ). The combustion efficiency factor was set to 0.8, and the net heat of combustion was set to 16.0 MJ/kg. The latter is considered as the lower heating value for moist wood, derived from the calorific value of 18.66 MJ/kg for dry wood [61] and a moisture content (dry value) of 14.5% [48]. The product of the combustion efficiency factor and the net heat of combustion is the effective heat of combustion.

The integration of MLR over the wood crib length was made by dividing the wood crib into 50 mm long elements and adding the MLR per unit length to all elements based on the start of burning for each element. The start of burning for each element was based on the fire spread across the wood crib found through video analysis. A curve of the total MLR was then found by summarising the MLR for all the 50 mm wood crib elements for each time unit (1 s). The primary assumption for this model is that the crib per unit length burns in the same way from ignition as the small wood crib on the scale.

The MLR for the CLT ceiling was determined from the average charring rate for each 10 mm into the wood, the density (484 kg/m^3)

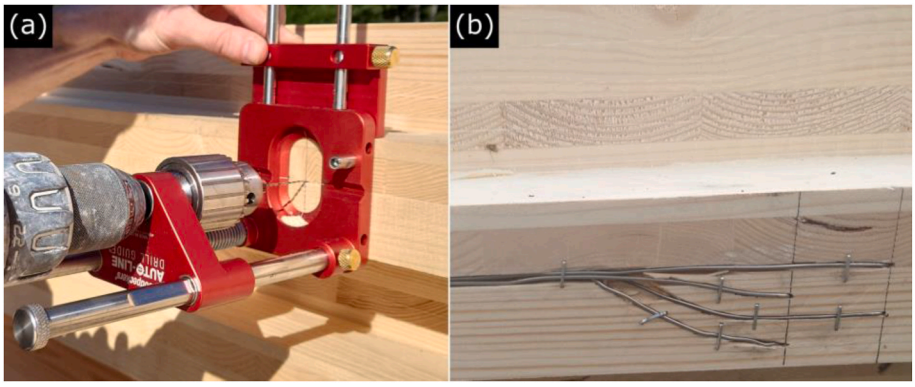

Fig. 7. (a) A drill guide was used to drill perpendicular holes into the CLT from the rebate joint. (b) The TCs embedded in the CLT were installed parallel to the isotherm in a zig-zag pattern.

and surface area (89.4 m^2) of the exposed CLT. The HRR was calculated with a combustion efficiency of 0.8 and a net heat of combustion of 16.3 MJ/kg. The higher heat of combustion is due to the lower moisture content of the CLT compared to the wood crib sticks.

2.4.3. Gas velocity measurements through bidirectional probes

Gas velocities were measured by bidirectional probes, as described in ISO 9705-1 Appendix D [55]. The velocities are here calculated similarly as by Ref. [4], originating from Ref. [62].

3. Results

3.1. Fire development

The wood crib was ignited, as described in Section 2.2.3. The heptane flames had a height of 1.0–1.5 m in the beginning and tilted towards the left end wall, away from the wood crib. This behaviour of the flames is believed to be due to local draft conditions. The heptane fire caused the formation of a thick black smoke layer below the ceiling across the entire compartment, and a slight discolouring was observed in the CLT ceiling closest to the left end wall. However, the ceiling did not ignite. The fire gradually decreased in size from around 2.5 min after ignition of the heptane, and the smoke layer was diluted. At 3.5 min, the heptane fire burned out, and the wood crib fire almost died out, with only 5 cm high flames over the first 5 cm length of the crib. During the next 30 min, the fire spread slowly and grew in size to cover about 1.5 m length of the crib, covering an area of approx. 3 m^2 and the crib fire base area stabilised at this size after 22 min, see Fig. 8. The base area of the fire was here defined as the length of the burning crib (i.e., the position of leading-trailing edge) multiplied by the width of the crib. The base area stabilised at approx. 3 m^2 because the fuel in the first part of the crib was burning out. The flame height during this period varied from 0.5 to 2.2 m, and flames were not impinging the ceiling, see Figs. 2 and 8.

At 32.5 min, the ceiling ignited above the wood crib fire. Thereafter, the fire took approx. 13 min to spread across the whole crib and cause a stable burning fire. Within these 13 min, the fire was travelling back and forth in four distinct cycles or waves, see Fig. 9. As we do not know of such behaviour being reported earlier, we have in this article chosen to name them *flashing waves*. The waves were characterised by a rapid flash fire below the ceiling, followed by a spread along the top layer of the wood crib, triggered by the intense radiation from the flames beneath the ceiling. Each wave caused external flaming out of the window openings. After a short, intense fire with a duration of 30–60 s, the flames underneath the ceiling were gradually reduced, and the radiation-dependent fire on the top layer of the wood crib was reduced or even extinguished in some areas. The flames underneath the ceiling spread almost to the end of the compartment for each wave. After the 1st and 2nd waves, the ceiling fire retracted entirely to full extinguishment (see Figs. 10 and 11). After each retraction, the wood crib fire had grown in both length and intensity compared to before the wave. The leading edge of the wood crib fire reached the end of the compartment in the 3rd wave (see Fig. 12). Despite the whole compartment burning, the fire pulled back again after a short period. Eventually, in the 4th wave, after 45:30 (mm:ss), all combustible surfaces in the compartment had ignited without any retraction. This stable burning of the whole compartment was defined as flashover.

After flashover, the fire burned intensely for about a minute and then gradually decreased in intensity. From 49 min on, the fire was clearly most intense at the right end, with small external flames emerging only from Window 4. The self-extinguishment of flames in the CLT ceiling started around 50 min from the left end (ignition end) of the compartment and continued towards the other end over the next 11 min, see Fig. 13. The wood crib fire was burning with continuous flames along the crib until 61 min. From 61 to 95 min, the wood crib fire was burning more and more discontinuously (i.e., with larger and larger areas of the crib without flames), starting from the left end of the compartment and moving rightwards. There were no visible flames from the wood crib after 95 min. The compartment was observed for a total of 4 h. At this point, very little of the wood crib was left, and some lamellas of the CLT were hanging down from the ceiling in the centre of the compartment. Hot spots were present around the delaminated areas. Manual fire suppression with water was then conducted, and no reignition was observed after the extinguishment.

After the compartment had cooled down, it was visually inspected, see Fig. 14. A few cracks at the surface of the gypsum boards were seen, but all of them remained in place. The inner gypsum board layer was undamaged except for some discolouring under the joints of the outer layer. The protected CLT back wall was undamaged.

A summary of the fire development is given in Table 1, while detailed information about temperatures, charring rates, mass loss rates, heat release rate, and external flames is found in the following sections.

3.2. Compartment temperatures

Temperatures below the ceiling, at the back wall and on top of the wood crib measured by PTs are shown in Figs. 15–17 and give an overview of the development of the fire. The first peak at 3 min originated from the heptane fire. After the extinguishment of the heptane fire, the temperatures slowly increased below the ceiling and at the upper part of the back wall due to the development of the wood crib fire. The maximum ceiling temperature reached a plateau between 22 and 33 min, which corresponds well with the almost constant fire base area for this period, see Fig. 8.

After 32.5 min, the ceiling spontaneously ignited. Temperatures in the entire ceiling increased rapidly but to a higher level near the ignition point and lower at longer distances. Increased temperatures were also measured at the wall, most pronounced at the upper part of the wall. In the figures, the retraction of the 1st flashing wave is recognised by a slight decrease in almost all temperatures except for the wood crib at X = 3.0 m, where the temperature continued to increase. In other words,

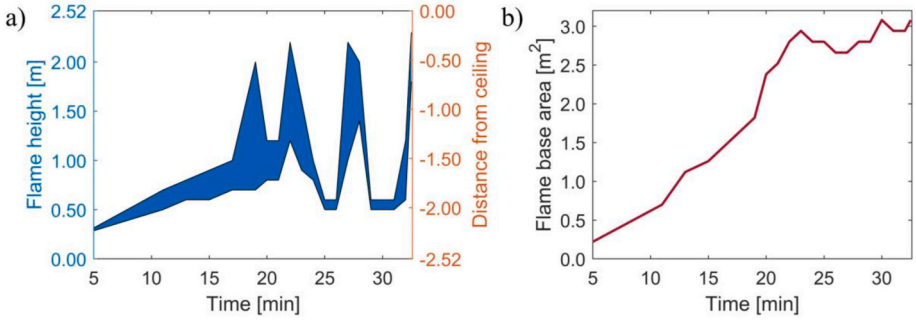

Fig. 8. (a) Flame height of wood crib fire. The shaded area represents the minimum and maximum height of the flame along the width of the crib. (b) Base area of wood crib fire before ignition of the ceiling.

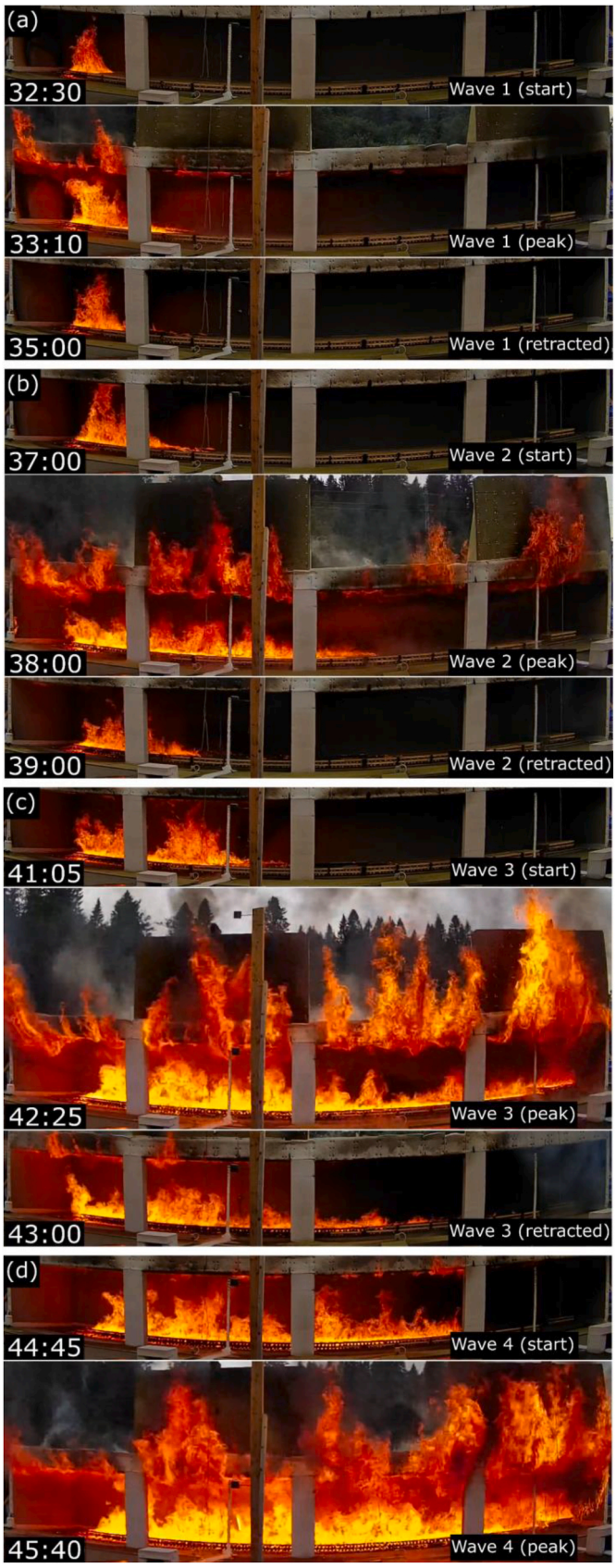

Fig. 9. (a), (b), (c) and (d) represent the 1st, 2nd, 3rd and 4th flashing waves, respectively. Time is given as (mm:ss) after ignition.

the wood crib fire during the 1st flashing wave spread beyond this point and did not retract. The wood crib temperatures farther away increased slightly and remained at this temperature until the next flashing wave. The 2nd flashing wave, see Fig. 9(b), started at 37 min and followed the same behaviour as the 1st wave. There were considerable temperature variations in the compartment during this period, with part of the compartment fully burning and the other part having temperatures close to ambient temperatures. After 42 min, the minimum compartment temperature also increased significantly, and the fire was at this point affecting the temperature in the entire compartment. This corresponds with the 3rd flashing wave, which led to the entire compartment burning, see Fig. 12. Although the fire retracted also after the 3rd wave, the wood crib fire grew substantially and covered more than half of the crib, and the temperatures of the non-burning parts remained high. The 4th wave occurred shortly after the end of the 3rd and led to a stable burning fire in the entire compartment. The highest temperatures were reached at 45–46 min, with the peak temperature of 1040 °C measured on top of the wood crib in the centre of the compartment.

The decay phase was initiated by a sudden drop in temperatures and continued with the extinction of flames in the ceiling. The extinction of flames started from the left side at approximately 50 min and continued to the right side. The last flames were gone at 61 min. During the extinction of the CLT, the oxygen concentration was 16–17% measured 100 mm below the top of Windows 2 and 4 (Fig. 25). The temperatures below the ceiling were 695–705 °C, corresponding to an incident heat flux of 49–52 kW/m^2. During the extinguishment of CLT, the average compartment temperature dropped from 910 °C to 650 °C.

The decay phase then continued almost linearly over the next 90 min, with an average temperature decay rate below the ceiling of 7.1 ± 0.5 °C/min. During the decay phase, there was little temperature difference along the Y-axis of the ceiling, i.e., between the window and back wall (Fig. 15). For the wood crib (Fig. 17), this difference was more pronounced, with the highest temperatures in the centre of the crib. The difference between the minimum and maximum compartment temperatures during most of the post-flashover and decay phase was between 200 and 400 °C.

During the 1st flashing wave, the thin paper of the gypsum boards ignited on the left end wall and the nearest part of the back wall, see Fig. 18. The maximum PT temperatures at the back wall close to the wood crib fire (X = 3.0 m) were 476 and 670 °C at 1.1 m and 2.4 m height, respectively. The corresponding maximum heat flux at 2.4 m height was 78 kW/m^2 and stabilised at 40 kW/m^2 until the next wave. At 1.1 m height, the maximum heat flux was 15 kW/m^2 before it reduced to approx. 10 kW/m^2 and slowly increased to 20 kW/m^2 before the second wave.

To better visualise the temperature variations in the compartment, temperature maps for the XZ and YZ cross-sections were made from the TC measurements through linear interpolation. In the XZ cross-section, see Fig. 19, strong temperature gradients were observed both in the X and Z direction. At locations where only the ceiling has ignited and not the wood crib, the temperature increased noticeably from the floor to the ceiling. However, for locations where both the crib and the ceiling had ignited, the lowest temperature was in the middle height of the room (Z ~ 1.0–1.8 m). The difference was as much as 300 °C between the coldest and the hottest regions. The highest temperatures were measured in the centre of the compartment with regard to X-axis, with temperatures above 1000 °C both below the ceiling (Z = 2.4 m) and above the crib (Z = 0.3 m). Such high temperatures occurred first at flashover and lasted only a few minutes. In the YZ-cross-section, see Fig. 20, there was a strong temperature gradient along the Y-axis. The temperatures were higher in the cross-section through Window 2 than Window 4 until the flames in the wood crib and CLT were extinguished.

The maximum temperature on the surface of the CLT behind the two layers of gypsum boards on the back wall was 106 °C. The maximum temperature at the glue line at 40 mm depth was 67 °C. The maximum temperatures for different depths into the wood were measured at

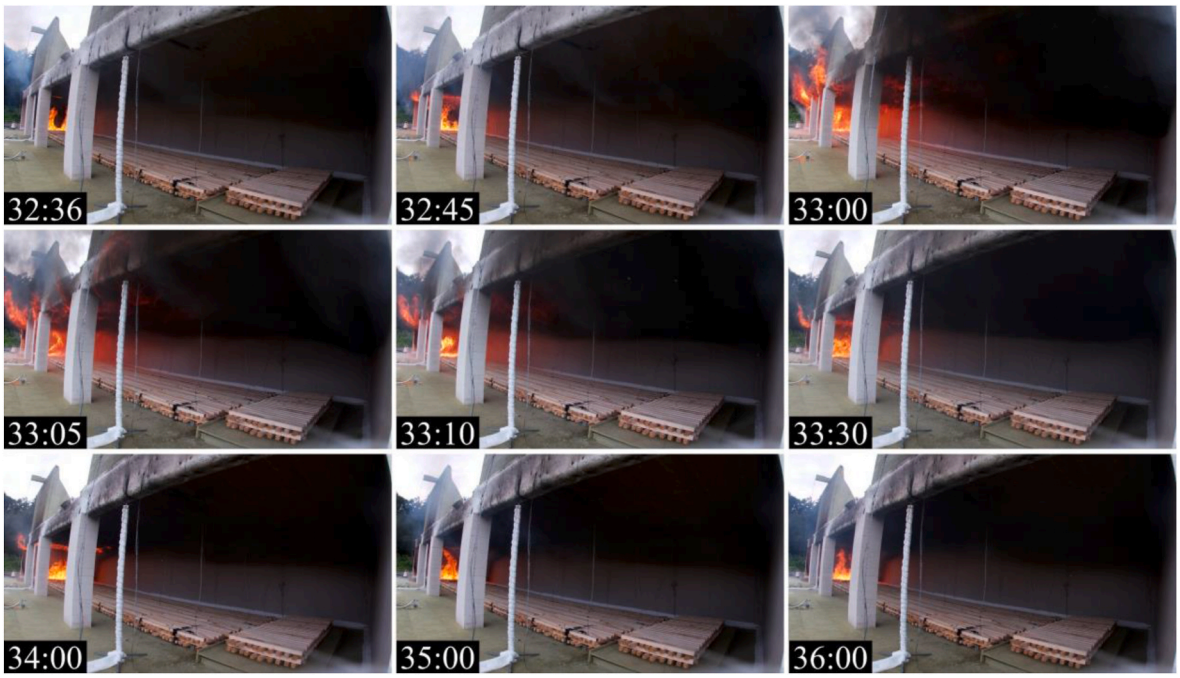

Fig. 10. Development of the 1st flashing wave. The ceiling ignites at 32:36, and within 30 seconds, flames reach almost to the end of the compartment. Flames retract after a short period. Time is given as (mm:ss) after ignition.

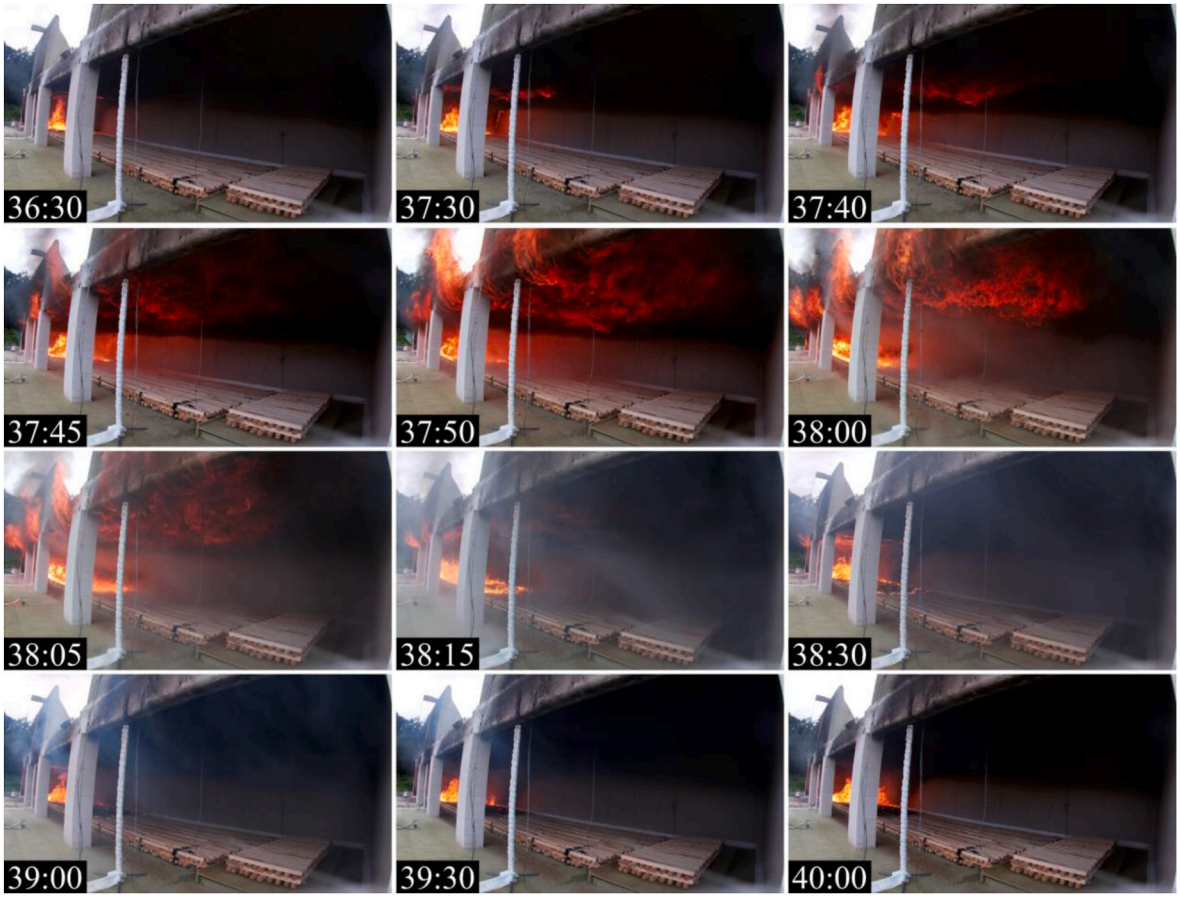

Fig. 11. Development of the 2nd flashing wave. At ~36:30, the ceiling reignites, and the flames spread below the ceiling by burning the combustible gases of the smoke layer. After a short, intense burning, the flames in the ceiling and top of the wood crib retract. Time is given as (mm:ss) after ignition.

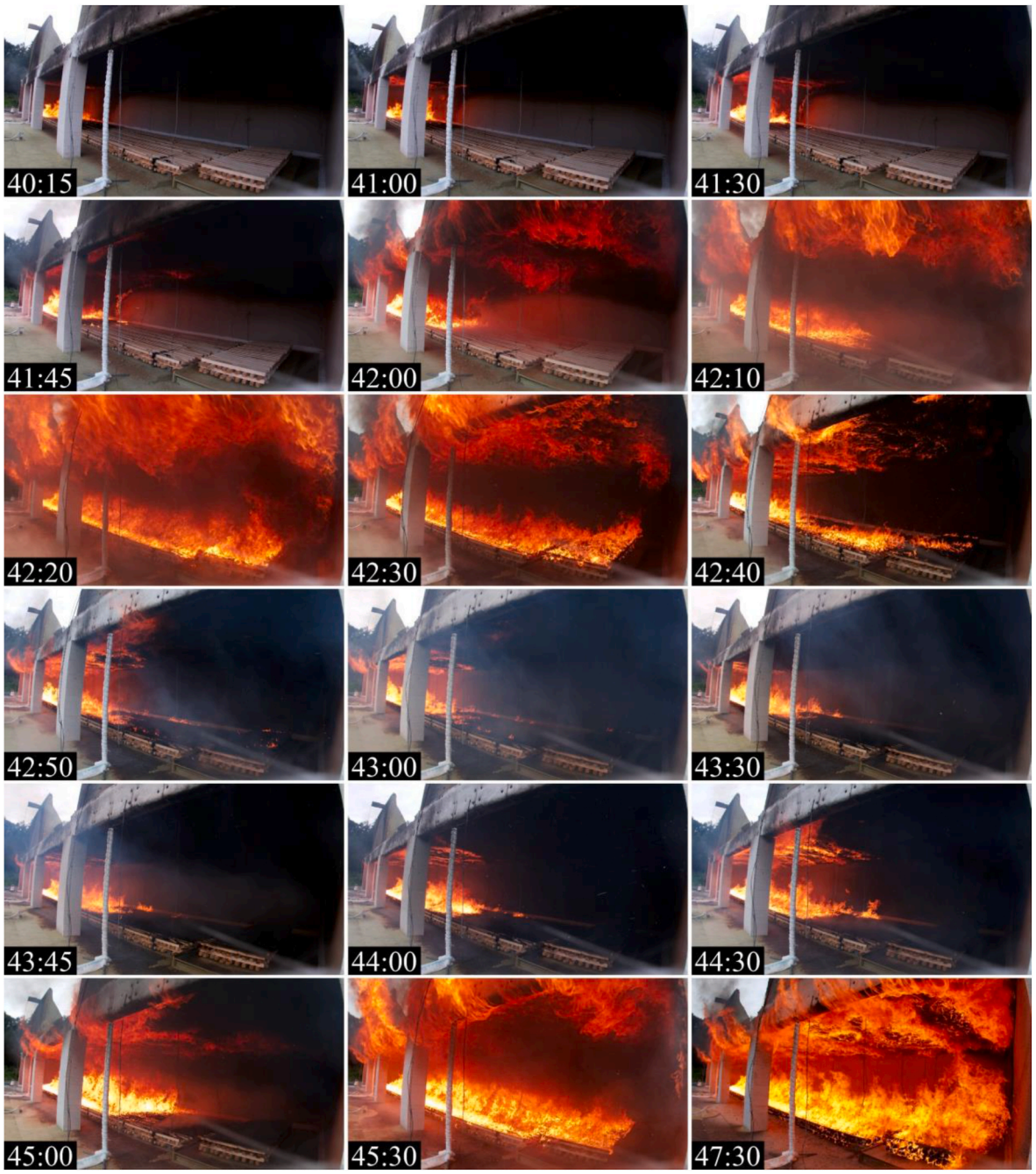

Fig. 12. Development of the 3rd and 4th flashing wave. Initiation of the 3rd wave occurs with reignition of the ceiling at ~40:15. Within 2 minutes, the flames have spread to cover the entire ceiling and crib. After a few seconds of the entire compartment burning, the flames below the ceiling and on top of the crib retract. The 4th wave occurs shortly after the retraction of the 3rd and leads to a stable flashover. Time is given as (mm:ss) after ignition.

125–140 min, i.e., more than 75 min after the most intense phase of the fire. After 300 min, the temperatures in the fire-exposed layer (0–40 mm) were almost uniform, at approx. 55 °C. These measurements were only from one position on the wall, i.e., X = 14.3 m and Z = 1.12 m.

3.3. External flames

External flames were present during the flashing waves and for a period of a few minutes after flashover. The largest flames exceeded the façade wall (i.e., flame height approx. 3 m above the window soffit) but were most of the time lower than the height of the façade wall. During the most intense external flaming immediately after flashover, the flames were approximately uniform for Windows 2, 3 and 4, while flames out of Window 1 were clearly smaller, see Fig. 9 (d). The external flames did in general not cover the entire window opening, see Fig. 9 (b–c).

The measured temperatures on the facades above Windows 2 and 4 are shown in Fig. 21. The temperature profiles above the windows were similar for the two windows but shifted slightly in time in relation to each other. This is because high temperatures were reached above Window 2 earlier than Window 4 as the fire was developing in this part of the compartment first. The temperature development above Window 4 had a more prolonged decay phase, as the crib at this end of the compartment burned out at last. Above both windows, four distinct short-lived peaks were observed, which correspond to external flames during the flashing waves.

Fig. 13. Cessation of flaming combustion in the ceiling occurred while the wood crib was still burning. Photo from 62 min.

Fig. 14. Compartment after burn-out of the wood crib. No gypsum boards had fallen down, and the wood crib was completely consumed.

The incident heat fluxes towards the façade above Windows 2 and 4 were calculated based on the PT and TC measurements, see Section 2.4.1, and are given in Fig. 22. The incident heat flux to the façade was highest during the flashing waves. For Window 2, the heat flux was at its highest during the 3rd and 4th wave, with a short-lived intensity of 20, 55 and 70 kW/m^2 at 2.8 m, 1.8 m, and 0.8 m above the window soffit, respectively. The large difference between 2.8 m and 1.8 m gives an indication of the height of the external flame.

For Window 4, the highest heat fluxes occurred during the 3rd flashing wave with a short-lived intensity of 60, 85 and 90 kW/m^2 at 2.8 m, 1.8 m, and 0.8 m.

After flashover, the heat fluxes were higher outside Window 2 until 50 min. From this point on, the heat fluxes were slightly higher above Window 4.

The size of the external flame was related to the gas flow velocity through the compartment windows. Gas flow velocities were calculated from the bidirectional probes, see Section 2.4.2, and are shown in Fig. 23. Characteristics of the experiment can be observed in the velocity profile for the gas flow through the windows. The first peak seen directly after the ignition of heptane was caused by smoke filling the upper part of the compartment and exiting out of Window 4. When the heptane fire was extinguished, the smoke layer vanished, and the gas velocity out from Window 4 was reduced to zero. In general, the flow out from

Table 1
Summary of the fire development.

Time [min]	Observation	Figure
0–3.5	Heptane trays are burning.	
3.5–32.5	Wood crib fire increases slowly in size, both with regard to flame height and area.	Figs. 2 and 8
32.5–33.5	**1**st **flashing wave**. The ceiling ignites without the wood crib flames impinging the ceiling. Fire spreads rapidly across the ceiling and partly across the wood crib.	Figs. 9 (a), Fig. 10
36.5–39	**2**nd **flashing wave**. Fire spreads again across the ceiling and the wood crib. External flaming out of all windows.	Figs. 9 (b), Fig. 11
41.5–42.5	**3**rd **flashing wave**. Fire spreads until the whole compartment is burning, with external flaming out of all windows. The ceiling fire retracts to approx. 9 m, and wood crib fire to approx. 11 m.	Figs. 9 (c), Fig. 12
45–45.5	**4**th **flashing wave**. Fire spreads to the end of the compartment for both the crib and the ceiling and causes a flashover without any retraction. Intense compartment fire with large external flames out of all windows.	Figs. 9 (d), Fig. 12
46–50	Fire intensity slightly reduced.	
50–61	**Self-extinction of CLT.** Intensity is reduced, and external flames are clearly smaller. Flames in the ceiling extinguish from left to right. Wood crib fire becomes more and more reduced, but there is still a continuous wood crib fire.	Fig. 13
61–95	Wood crib fire burn discontinuously, starting from the left end and moving right.	Fig. 13
95–240	Decaying temperatures, no visible flames, and no re-ignition.	Fig. 14

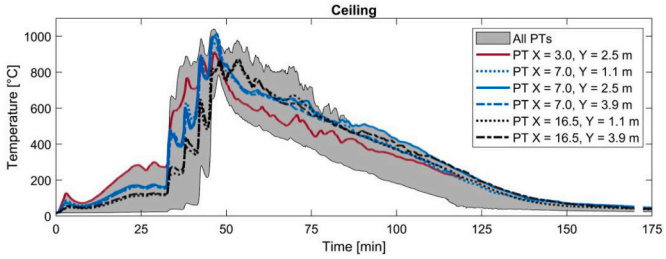

Fig. 15. Temperatures 100 mm below the ceiling measured by PTs facing downwards. The grey area covers all measurements by PTs in the compartment. X and Y represent the position of the PTs.

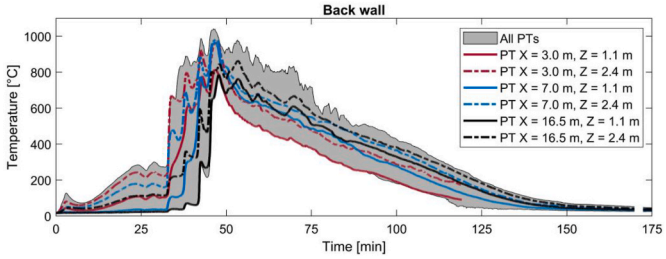

Fig. 16. Temperatures 100 mm in front of the back wall measured by PTs facing away from the wall. The grey area covers all measurements by PTs in the compartment. X and Z represent the position of the PTs.

Window 4 was higher than for Window 2. The flow out from Window 2 peaked at 10 m/s at 47 min before it dropped significantly and then again at 49 min. This corresponds with the observations of no external flaming out of this window. The velocity through Window 4 increased to a maximum of 12 m/s at 52 min and thereafter gradually reduced. The flow into the compartment slowly increased through Window 2 from ignition, while the flow through Window 4 was zero until flashover. An

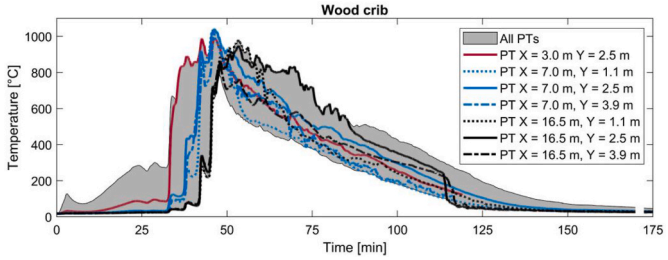

Fig. 17. Temperatures on top of the wood crib measured by PTs facing upwards. The grey area covers all measurements by PTs in the compartment. X and Y represent the position of the PTs.

Fig. 18. During the first flashing wave, the heat exposure to the walls was sufficient to ignite the paper of the gypsum boards on the walls close by.

increase in inflow velocities occurred through both windows at flashover but with the highest velocity through Window 2.

3.4. Fire spread across ceiling and wood crib

The fire spread across the ceiling and the wood crib is shown in Fig. 24, where the spread was slow until the ignition of the ceiling. Thereafter, the spread was dominated by the four flashing waves. The waves were always initiated by a spread across the ceiling first, shortly followed by a spread across the wood crib. The flames under the ceiling travelled almost to the end in the first two waves and reached the end in the final two waves. The leading edge of the flame spread remained at its maximum position just a few seconds before the flames retracted, starting in the ceiling. The ceiling fire retracted completely after the two first waves, while the wood crib fire grew larger after each wave. An exponentially increasing curve gave a good fit to the fire spread across the wood crib when the flashing waves were filtered out. The derivative of the fitted curve was then used to estimate the fire spread rate across the wood crib. Before the ceiling was ignited at 33 min, the fire spread rate in the crib increased from 0 to 3 mm/s, with an average rate (harmonic mean) of 0.9 mm/s (54 mm/min). After this point, the spread rate increased from 3 mm/s to 60 mm/s over the next 13 min, with an average spread rate of 20 mm/s (1.2 m/min). The fitted curve was also used to estimate the wood-crib total mass loss rate and HRR (see Section 3.5). No fitted curve was made to the fire spread across the ceiling due to the immense effect of the flashing waves. However, as seen in Figs. 10–12, the flames below the ceiling travelled across the compartment in 60 ± 30 s during the flashing waves.

3.5. Gas measurements

The concentration of oxygen (O_2), carbon monoxide (CO) and carbon dioxide (CO_2) were measured at three different locations as described in Section 2.3. The results are shown in Fig. 25. The O_2 concentration was about unchanged until the ceiling ignited. Thereafter, O_2 decreased in a pulsating way corresponding to the flashing waves. The lowest O_2 measured was approx. 9% and 12.5% at flashover in Windows 2 and 4, respectively. After this point, the O_2 increased steadily. The increase was faster in Window 2 compared to Window 4, which corresponds with the earlier extinguishing of the CLT in this section. The lowest O_2 at the back wall was slightly below 19%. However, the measurement at the back wall was higher than expected and may have been caused by a leakage in the tube collecting the gas.

The CO_2 concentration increased with approximately the same percentage as the oxygen decreased. The concentration of CO increased significantly after the ignition of the ceiling, and the highest levels were measured during the flashing waves. Between 37 and 51 min, the CO levels increased above the measuring range of the sensors, 5000 ppm, and are therefore unknown. After 53 and 60 min, the CO levels increased in Windows 2 and 4. This is related to the extinction of flames in the CLT and indicates that smouldering is still ongoing, producing CO.

3.6. Charring of CLT ceiling

After the experiment, the final char depth was measured through the method explained in Section 2.3. The results are shown in Fig. 26, with a dark green marking for the areas with the smallest char depths and dark red for the most considerable char depths. The arithmetic average of the char depth was 26 mm with a standard deviation of 4 mm, corresponding to an approximate mass loss of 1125 kg. The char depth was strongly non-uniform, with the most severe charring from the centre of the ceiling towards the right side of the compartment, and less charring at the left side of the ceiling, although this part had the longest fire duration. The char depth was also larger near the back wall than near the window wall. This was observed along the whole length of the compartment.

In the centre of the compartment where the final char depth was largest, see Fig. 26, some delamination of the 1st layer had occurred. This is shown in Fig. 27(a), where several lamellas were partly loose and hanging from the ceiling and clearly detached from the layer behind. We refer to this behaviour as delamination, although the lamellas apparently had not detached along their entire length. Delamination occurred, although the char depth had not reached the first glue line in the CLT. This was caused by the temperature in the glue line exceeding the operational temperature of the glue and adhesion between the glue and the timber was therefore lost. Shortly before the experiment was terminated and extinguished, it was examined with an infrared camera. Some hot spots were detected behind the loose lamellas and next to the glulam beam, indicating that charring was still ongoing.

The temperatures at the glue-line interface were at maximum 194, 180 and 164 °C at location X = 4.7, 9.5 and 14.3 m and were reached after 120 min, more than an hour after the maximum compartment temperatures. These temperatures corresponded well with the observation that the visible lamellas of the 2nd layer were mainly discoloured and not charred (Fig. 27(a)).

Fig. 27(b) shows charring at one of the locations where the charring rate of the CLT was measured. The char depth was between 20 and 30 mm at this location. No signs of a corner effect at the CLT joints were observed, although the TCs were installed from the rebate joint.

Charring rates of the CLT are given in Table 2 and calculated from the embedded TCs at 0, 10, 20, 30 and 40 mm depths into the CLT and the final average char depth measured after the experiment, see Section 2.3.

Charring was defined to start when the CLT burned continuously, i.e., the short burning periods during the flashing waves were neglected.

3.7. Mass loss rate and heat release rate

The wood-crib mass loss and mass loss rate during the fire experiment were determined as described in Section 2.4.2. Due to overheating of the scale during part of the experiment, data were lost from 50 to 75 min. A decaying exponential curve was fitted to the existing data.

The MLR per unit length (50 mm) was found by derivation of the mass loss curve of the small crib and divided by 20 to convert the numbers from 1 m length to the unit length. The results are shown in

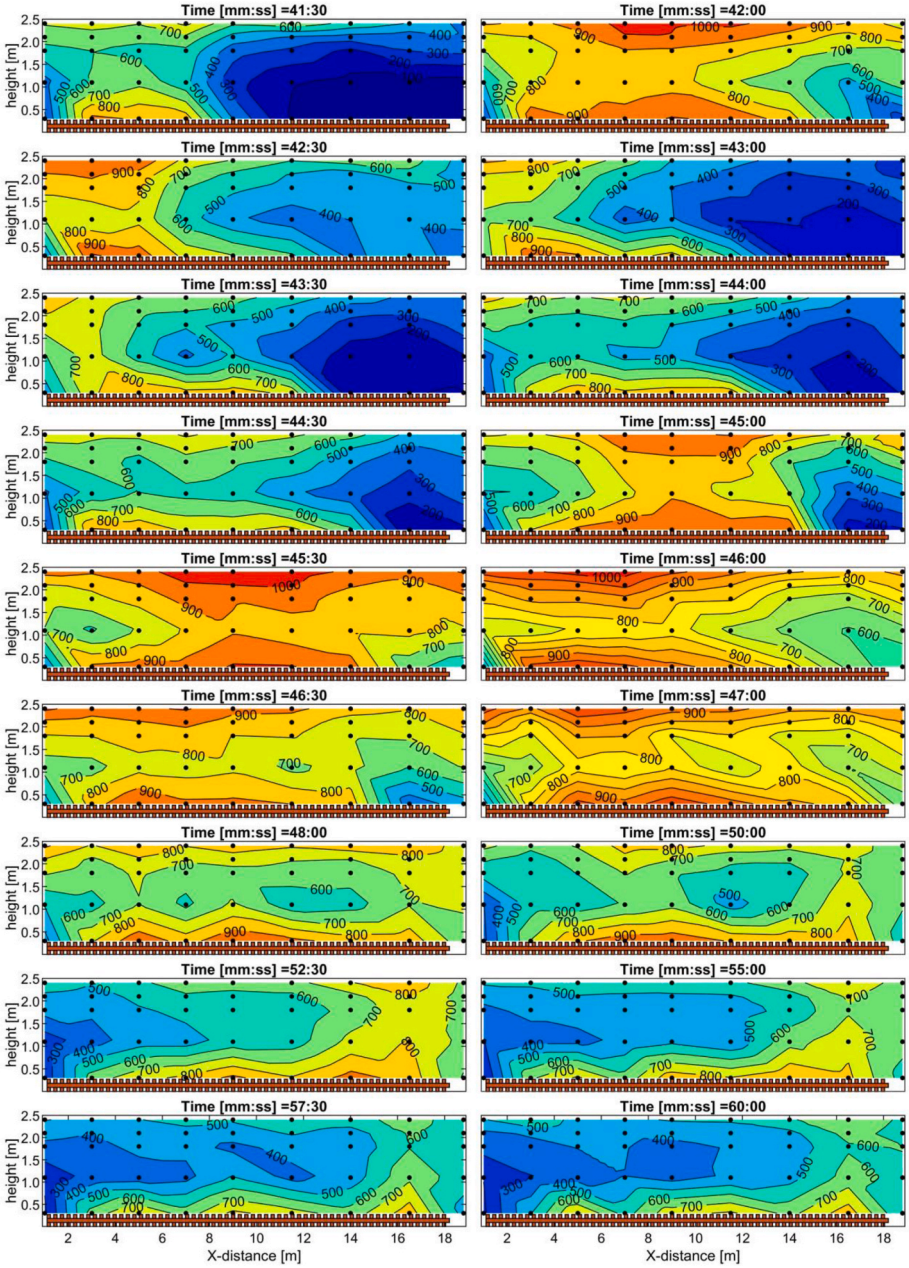

Fig. 19. Temperature maps of the cross-section through the XZ-plane at Y = 2.5 m. The black dots represent the positions of the TCs. The maps show the progression of the 3rd flashing wave (41:30–42:30), 4th flashing wave (45:00–45:30) leading to flashover (45:30) and the start of the decay phase with the extinguishing of the CLT (50:00–60:00).

Fig. 28.

The total MLR, for large and small crib combined, was obtained by combining the fire spread across the wood crib (Fig. 24) and the MLR per unit length shown in Fig. 28. An illustration of this method is given in Fig. 29. The estimated maximum MLR for the crib was 1.53 kg/s, which is converted to 4.14 g/(s m^2), in terms of the surface area of the wood sticks. The MLR of the crib was enhanced by the thermal feedback from the compartment, and a lower value would, therefore, be expected for a similar crib fire in open air.

The estimated MLR of the CLT was found based on the charring rates in Table 2, see Section 2.4.2. The MLR was at its maximum 1.61 kg/s, corresponding to 18 g/(s m^2).

The HRR is shown in Fig. 30. The HRR of the crib is at maximum 20 MW. The curve has a sharp peak, with a steeper increase than decrease. The HRR of the CLT has a stepwise pattern as it was based on the charring rates. The step values are 21.0, 10.5 and 3.5 MW. The total HRR has a peak value of 41 MW, which equals a HRR per unit floor area of 436 kW/m^2. From the ignition of the ceiling, the HRR development has a growth rate between the fast and ultrafast t^2-curve [45].

The area under each HRR curve gives the energy released for the wood crib, the CLT and in total. Since a combustion efficiency of 0.8 was used, the area should ideally correspond to 80% of the energy content of the initial wood crib mass (2065 kg) and the mass of the burned CLT (1125 kg), which equals 33.0 GJ and 18.3 GJ for the CLT. The area below the HRR curve for the wood crib was 82% of the energy content of the initial wood crib, while the area below the HRR curve for the CLT was equal to 97% of the energy content of the mass of burned CLT.

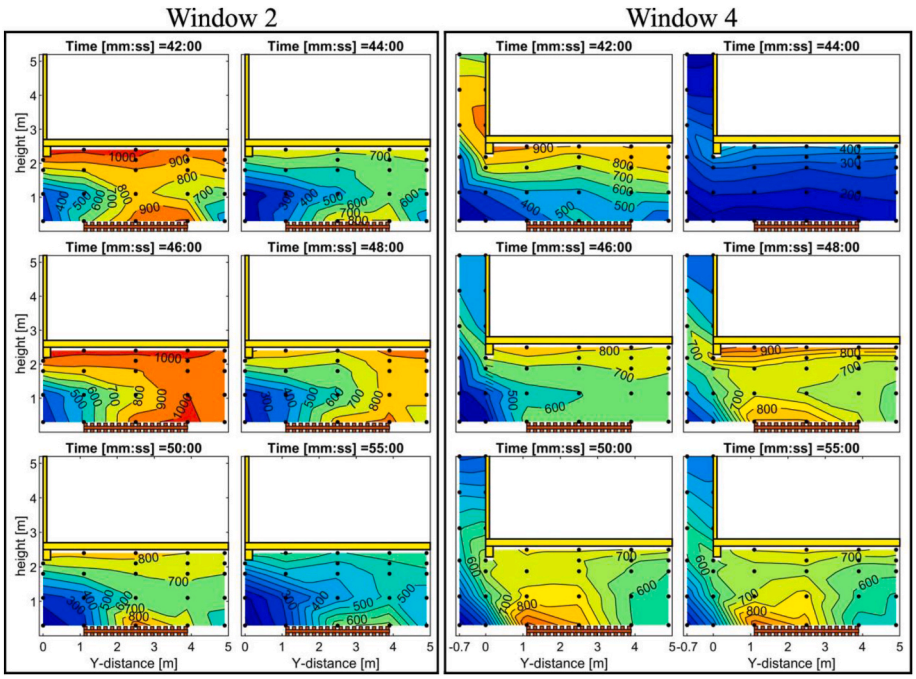

Fig. 20. Temperature maps of the cross-sections through the centre of Window 2 (X = 7.0 m) and Window 4 (X = 16.5 m) during part of the 3rd flashing wave (42:00), flashover (46:00) and the start of decay phase (50:00–55:00). The black dots represent the positions of the TCs. Temperatures for the outside area are missing for Window 2 due to a logger failure.

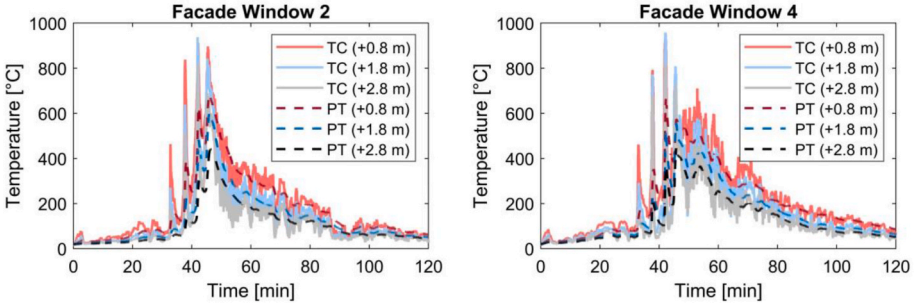

Fig. 21. Temperature measurements at the façade above Window 2 and Window 4. + 0.8, 1.8, 2.8 m are the heights above the window soffit.

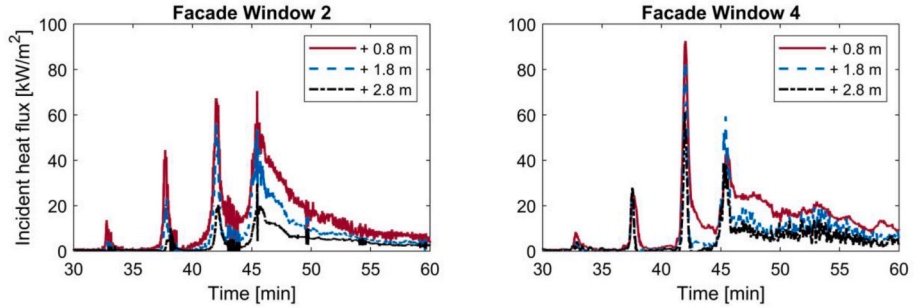

Fig. 22. Incident heat fluxes above Windows 2 and 4 calculated from PT and TC measurements at the façade above Window 2 and Window 4. + 0.8, 1.8, 2.8 m are the heights above the window soffit.

4. Discussion

4.1. Fire spread

The fire spread can be divided into two phases, before and after the ignition of the ceiling. In the beginning, the fire spread was slow for several reasons; the flames reached 0.5–2.2 m above the floor but were not impinging the ceiling, and surfaces with non-impinging flames require a higher heat flux to ignite than surfaces with an impinging flame [63]. In addition, due to open windows and only a 0.36 m deep reservoir created by the glulam beam, a thick smoke layer was not able to form. Hence, the radiation towards the ceiling was not sufficient to ignite the CLT. The slow fire spread before the ignition of the ceiling is a good indicator of how the fire would have continued to spread if the CLT

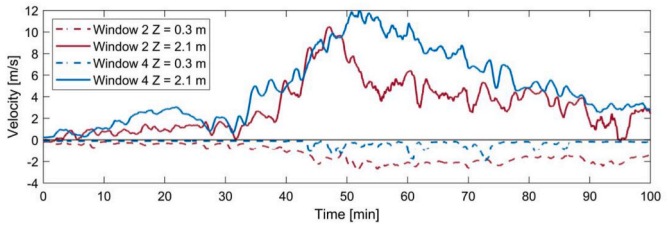

Fig. 23. Gas flow velocities in and out of Windows 2 and 4. The values are averaged over 30 s. Positive values represent outward flow, and negative values inward flow.

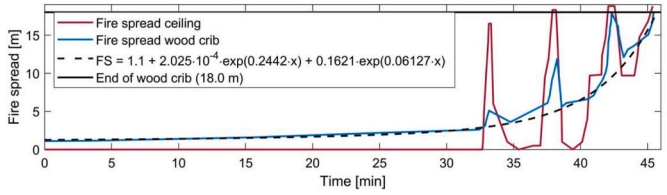

Fig. 24. Fire spread across the wood crib and the CLT ceiling.

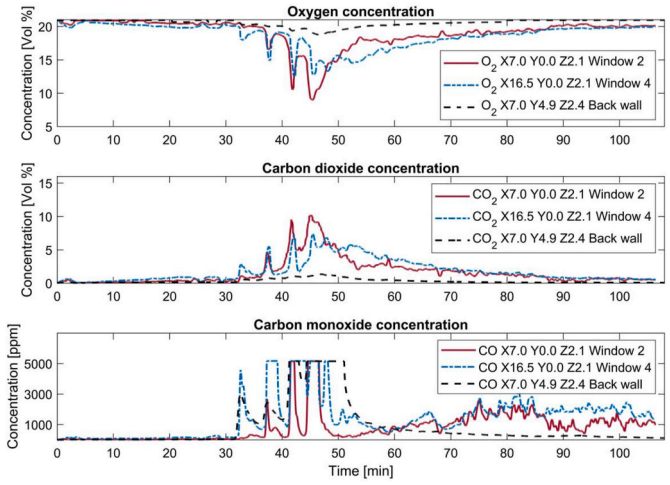

Fig. 25. Oxygen (O_2), carbon monoxide (CO) and carbon dioxide (CO_2) concentration.

ceiling had been protected or not present. This is in line with other travelling fire experiments with a similar wood crib, geometry and ventilation conditions [30,35]. Fire behaviour in such conditions could be explained by the theoretical model called "Weak-plume localised fire" [64].

The ceiling was ignited at around 33 min by a combination of hot smoke and radiation from the flames. The late ignition of the ceiling compared to the CodeRed experiments [17,36] is an important observation which is relevant for the fire safety design of CLT compartments with a low likelihood of ceiling-impinging flames (e.g. with a high ceiling) and a low potential for collection of combustible gases under the ceiling, e.g. compartments with ceiling beams of limited height and high ventilation openings.

From the ignition of the ceiling, the fire dynamics changed completely, and the fire spread was significantly faster. A characteristic behaviour in this experiment was the flashing waves, in which the flames travelled back and forth several times. Although the fire retracted after each wave, the wood crib fire grew larger. The temperatures in the compartment increased as well after the retraction of each wave, including locations far away from the wood crib fire, despite the compartment being well-ventilated. Thus, the combustible materials in the wood crib and ceiling farther away from the ignition source were preheated and, therefore, more prone to ignite at a later point. This can explain the shorter and shorter durations between the flashing waves.

The temperature profiles adapted well to the visual impression of the flames during both the flashing waves and flashover. For instance, the lowest temperatures were present at a height of 1.0–1.8 m above the floor in the most intense burning phase, which can be explained by the absence of flames at this height. It was burning both in the ceiling and above the wood crib, but none of these flames reached the middle height of the room.

The fire spread rate corresponded well with an exponentially increasing curve. Thus, the maximum and the average fire spread rates would likely have been higher if the compartment had been longer. Flashing waves have not been reported from any other research on travelling fires, but a localised flash without the retraction is called a "Zonal Intense Burning" [64].

The flame spread direction in both the ceiling and across the wood crib was directly influenced by the glulam beam. Although the glulam beam only reached 0.36 m below the ceiling, it created an effective barrier for the smoke to exit out of the closest window. Hence, the smoke was instead effectively guided towards the other end of the compartment, where it exited out of Window 4 as the smoke layer filled up the volume entrained by the glulam beam. This explains the higher outward flow velocities through Window 4 compared to Window 2 before ceiling ignition. When the ceiling ignited, it had already been preheated for a while. This contributed to a fast flame spread across the ceiling. With the burning ceiling, and the intense radiation onto the wood crib, the wood crib fire also started to spread. As the wood crib was already burning, the spread could be considered a piloted ignition. The slower fire spread across the wood crib compared to the ceiling can be explained by the crib being less preheated before the spread took place. Several of the characteristics of this experiment, including the rapid flame spread

BACK WALL

Y \ X	0.2	0.7	1.2	1.7	2.2	5.0	5.5	6.0	6.5	7.0	9.8	10.3	10.8	11.3	11.8	14.5	15.0	15.5	16.0	16.5	16.8	17.3	17.8	18.3	18.8	AVG
4.8	21	27	24	22	24	31	27	24	22	24	30	32	33	33	32	33	32	33	30	29	29	26	25	25	27	28
4.3	22	25	22	19	27	22	25	22	19	27	24	30	32	36	27	25	28	27	30	28	30	29	23	22	27	26
3.8	23	23	24	25	29	23	23	24	25	29	27	33	32	28	26	25	32	29	30	33	29	27	24	23	25	27
3.3	27	24	25	22	29	27	24	25	22	29	27	33	27	32	27	25	32	34	32	31	29	28	22	23	25	27
2.8	26	29	22	22	26	26	29	22	22	26	30	30	30	28	26	38	35	36	29	32	30	30	24	24	28	28
2.3	30	26	26	20	27	30	26	26	20	27	28	28	30	32	28	29	30	28	28	31	27	28	25	23	23	27
1.8	25	27	24	22	23	25	27	24	22	23	21	30	32	31	30	27	29	28	28	31	26	27	25	25	21	26
1.3	22	23	20	22	25	22	23	20	22	25	22	24	28	32	26	26	30	33	29	26	24	24	21	22	22	24
0.8	24	22	20	22	21	24	22	20	22	21	19	25	27	27	20	23	31	25	26	25	23	22	21	23	21	23
0.3	20	21	22	24	22	20	21	22	24	22	28	26	26	32	24	40	27	30	31	25	22	26	24	26	24	25
AVG	24	25	23	22	25	25	25	23	22	25	26	29	30	31	27	29	31	30	29	29	27	27	24	23	24	

IGNITION SIDE

WINDOW WALL

Fig. 26. Final char depth [mm] presented as a 2D plan view of the CLT ceiling. The bold numbers at the left side and top represent the X and Y locations [m] given in Fig. 5.

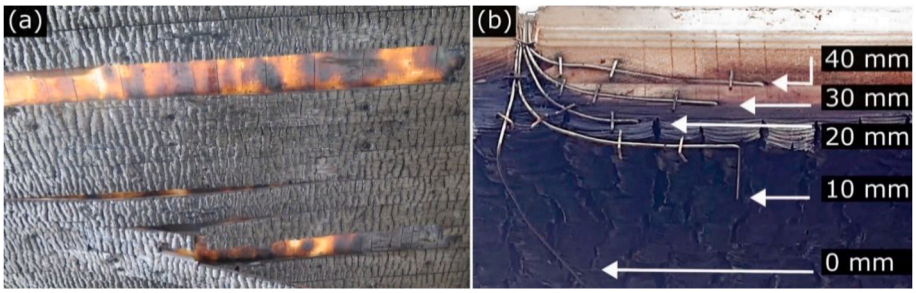

Fig. 27. (a) Examples of delamination of the CLT ceiling. (b) Example of charring close to the TCs embedded in the CLT. The 0 mm TC was attached to the surface of the CLT and was used to define the onset of charring at this point.

Table 2
Onset of charring at different depths, and charring rates of CLT ceiling.

Location	Time to reach 300 °C [min]					Charring rate [mm/min]				
	0 mm	10 mm	20 mm	26[a] mm	30 mm	0–10 mm	10–20 mm	20-26[a] mm	20–30 mm	0-26[a] mm
X 4.7 m	37.6	43.1	52.3	–	81.2	1.81	1.36	0.35	0.35	1.02
X 9.5 m	41.5	45.2	59.8	–	–	2.69	1.09	–	–	1.13
X 14.3 m	45.2	49.7	66.8	–	–	2.21	0.93	–	–	1.26
Average	41.4	46.0	59.6	77.0[b]	–	2.23	1.13	0.35	–	1.13

[a] 26 mm is the average final char depth of the CLT ceiling.
[b] 77 min is the time to reach 26 mm based on the charring rate between 20 and 30 mm at X 4.7 m and the average time to reach 20 mm char depth.

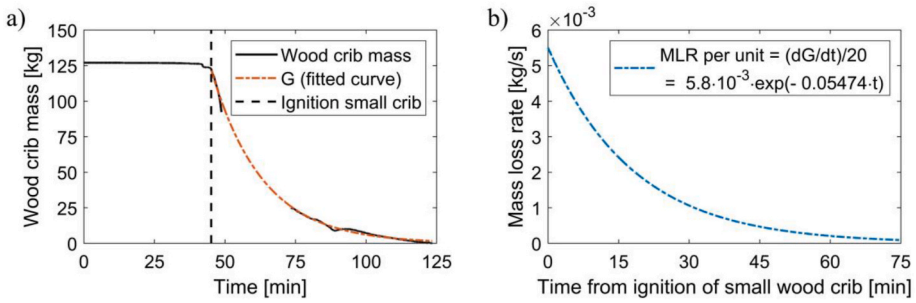

Fig. 28. (a) Mass change of the small wood crib (1.0 m × 2.8). (b) Mass loss rate per unit length (50 mm) of the small wood crib.

underneath the ceiling and the increased fire spread rate of the wood crib after ignition of the ceiling, were also observed by Nothard et al. [34]. The geometry, opening factor and moveable fuel of the experiment are comparable, except that their experiment was smaller in scale.

The fire spread rate after ceiling ignition was on average 1.2 m/min (20 mm/s) across the wood crib, which is considerably slower than the spread rate across the crib in the CodeRed experiments, with an average spread rate after ignition of the ceiling of 9.6 m/min (160 mm/s) in CodeRed #01 and 9.0 m/min (150 mm/s) in CodeRed #02. However, the wood crib in those experiments was made of 30 mm × 30 mm wood sticks and 5 mm thick wood fibreboard strips. Despite a larger distance between the wood crib and the ceiling (~2.7 m), the flames were impinging the ceiling. Hence, the setup was designed for a faster combustion and had an average spread rate of 0.6 m/min (11 mm/s) even before the ceiling was ignited. These differences highlight that the type of fuel and whether the flames are impinging the ceiling greatly impact the fire spread rate.

4.2. Flashing waves

A characteristic flame behaviour in this experiment was the flashing waves. Fires have been observed to travel back and forth in large compartments earlier [38], although at a completely different rate and caused by the lack of oxygen. Hence, the behaviour observed in this experiment has not been reported earlier, to our knowledge. The mechanisms behind this phenomenon can be explained by the general extinction theory for flames [65] and are related to the self-extinction of flaming combustion of CLT [66–68] and the feedback reaction between the wood crib and the exposed ceiling.

All the flashing waves started with ignition of the CLT ceiling above the existing wood crib fire. Since the ceiling had been preheated before ignition, the initially small flames from the ceiling grew rapidly to cover a larger area. The burning CLT was then able to ignite the combustible gases of the smoke layer, which had filled the entire reservoir created by the glulam beam. From Figs. 10–12, it is apparent that the main driving force for the flame spread below the ceiling was burning of combustible gases in the smoke layer. The combustible gases were likely produced by heating of the CLT, as emission of combustible gases are known to occur from CLT, or wood in general, before it ignites. Some combustible gases were also likely due to inefficient burning of the wood crib and the CLT.

The flames beneath the ceiling caused a high heat flux towards the wood crib, which enlarged the existing wood crib fire and caused the fire to spread along the top layer of the wood crib.

The retraction of the flames started at the far end of the compartment. Here, the flames beneath the ceiling had predominantly been supplied by combustible gases produced at the other end of the compartment. A few seconds after ignition of the CLT, the pyrolysis gases produced before ignition had been combusted, and only combustion of pyrolysis gases produced continuously was ongoing. This transition caused a natural reduction in flame size.

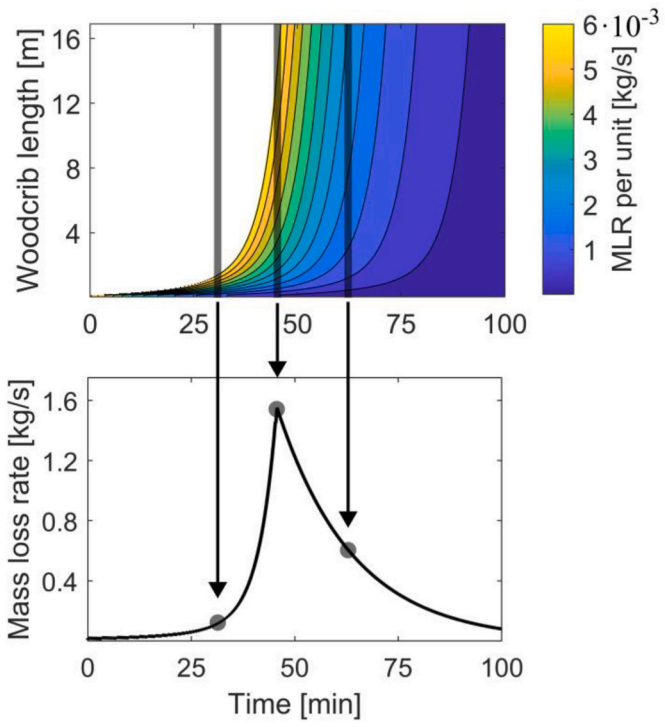

Fig. 29. Illustration of how the mass loss rate for the whole wood crib was determined. At the top, the MLR per unit length is represented by contour lines as a function of time and wood crib length. The curve is a combination between Figs. 24 and 28. By summation over the MLR per unit length for all wood crib units at one time point (illustrated by grey lines), the MLR for the given time point is generated (grey dots).

Moreover, the external heat flux to the ceiling decreased with increasing distance from the initial wood crib fire, caused by two mechanisms: Firstly, close to the initial wood crib fire, the radiation to the ceiling was high due to the well-established wood crib fire. However, with increasing distance from the initial wood crib fire, mainly the top layer of the crib was burning, and the radiation to the ceiling was strongly reduced. Secondly, farther away from the initial wood crib fire, a larger fraction of the heat produced was used to heat the air and surrounding materials, as these had been preheated less than materials and air closer to the initial wood crib fire.

Summarised, the extinction and retraction of the flames at the leading edge were due to too low supply of new combustible gases to sustain burning after the combustible gases of the smoke layer had been consumed. The low supply of combustible gases can be explained by the low temperatures of the compartment and the CLT. At X = 16.5 m, the PT temperatures below the ceiling were at maximum 270 °C, 436 °C and 645 °C during the 1st, 2nd, and 3rd flashing waves, respectively.

Extinction of flames might also occur if the oxygen concentration is reduced below a critical level depending on temperature [65]. The minimum oxygen concentrations at X = 16.5 m were 18.0%, 14.9% and 12.5% during the 1st, 2nd, and 3rd flashing waves, respectively. These values are higher than the critical oxygen concentration for sustained burning [65], and the contribution from the oxygen concentration seems to play a minor role here.

Usually, a wood crib fire is able to sustain burning on its own without any external heat flux [49]. However, since mainly the top layer of the crib was burning, the combustion was highly dependent on the external heat flux. With the retraction of the flames below the ceiling, the incident heat flux towards the wood crib was reduced to a level which no longer could sustain combustion, and the wood crib fire retracted as well.

Despite the retraction of the flames, the temperature maintained at a higher level than before the flashing waves, as seen in Figs. 15–17. This higher temperature preheated the material, which led to shorter and shorter times between the flashing waves, and the flashing wave increased in intensity and duration for each new wave, see Figs. 10–12.

4.3. *Self-extinguishment of flames in CLT*

Self-extinguishment of CLT when the variable fuel has burned out is an important factor for safe implementation of CLT in buildings [66]. This has been observed in several CLT experiments [17,18,36] and was also observed in this experiment.

After flashover, the whole ceiling burned for only a few minutes before extinction started from the left side after around 50 min and was completely extinguished after 61 min. Extinction of the flames in the CLT after flashover was recognised by a significant drop in the average compartment temperature after 50 min, followed by an almost linear decay curve. The relatively long extinguishing time aligned with the time the fire travelled across most of the wood crib. This indicates that the heat flux to the ceiling from the wood crib reached a critical level to sustain the flaming combustion of the CLT. The CLT was extinguished at a PT temperature of 695–705 °C and heat fluxes of 49–52 kW/m^2. This is slightly higher than the suggested critical heat flux of 43.6 ± 4.7 kW/m^2 for the same wood type in small-scale experiments [13]. Nevertheless, the fact that extinguishment of the flames occurred at similar temperatures and heat flux levels indicates that the extinguishment of CLT can be predicted based on the temperature in a compartment fire.

The PT temperatures related to extinction were higher than extinction temperatures when considering the XZ temperature map (Fig. 19). However, this can be explained by using TCs instead of PTs, as PTs are generally more exposed to radiation from the surroundings than TCs.

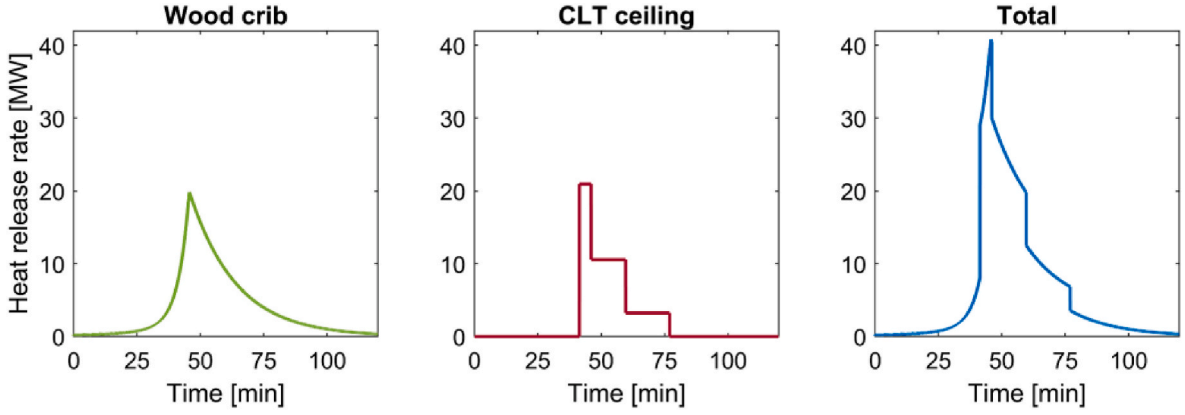

Fig. 30. Estimated heat release rates of the wood crib and the CLT ceiling.

4.4. Charring rate and heat release rate

The charring rate of the CLT varied significantly from the first 10 mm to the subsequent 10 mm intervals. The charring rate for the first 10 mm was 2.23 mm/min (Table 2), which is higher than values often reported for average charring rates of CLT [44,69]. The average charring rate over the entire CLT char depth of approx. 1 mm/min (Table 2), on the other hand, is in line with the average charring rates reported earlier [44,69].

Mitchell et al. [44] reported that high charring rates are related to large openings, which can be explained by increased charring with high oxygen concentrations [70]. However, the high charring rates for the first 10 mm followed by reduced charring rates are here instead believed to be caused by a combination of the natural mass loss rate variation found in wood and the significant variations in temperature and heat fluxes during the experiment, which are known to influence the charring rate [70]. The natural mass loss variations in the wood are clearly shown by looking at a typical mass loss rate curve for wood in a cone calorimeter experiment, where there is an initial peak in the mass loss rate directly after ignition, followed by a reduced but stable mass loss rate [71]. This behaviour is due to the formation of a char layer that works as an insulation layer to the uncharred wood.

As the charring rate is related to the HRR, the high initial charring rate also led to a high initial HRR peak. Although this high HRR only lasted a few minutes, the contribution from the CLT to the HRR during this period was significant. It will be a driving force for increased fire spread and large external flames and should not be neglected.

The stepwise pattern of HRR for CLT, see Fig. 30, is obviously not accurate. However, it gives a good representation of the actual curve, although a shorter distance between the embedded TCs would have given an even more realistic curve. Nevertheless, we consider this presentation of the HRR to be a better approach than presenting the HRR as a constant value between the start and end of charring. As an example, in the CodeRed-experiments, the contribution from the CLT was reported to be similar to the wood crib based on a constant HRR contribution from the CLT [17]. With the strongly varying HRR measured in this experiment, it is safe to assume that the HRR of the CodeRed-experiments also changed through the fire. Hence, the peak HRR for the CLT in the CodeRed-experiments was likely higher than for the wood crib in the most intense phase of the fire.

The MLR of the wood crib was based on the measured mass loss of the small wood crib. As the small crib was elevated 0.2 m higher than the large crib, it was positioned at the end of the compartment to not influence the fire spread across the wood crib. In addition, it was easier to protect signal wires from heat when positioned at the end than if it had been in the centre.

The wood crib burning before ignition of the ceiling likely burned with a lower maximum MLR than assumed from the calculations, as the re-radiation from the surfaces to the crib was minimal before ignition of the ceiling. However, the part of the crib burning before the ceiling ignited was relatively small compared to the whole crib, and we have neglected this difference in calculation of the total MLR for the whole crib. From the point the ceiling was ignited, the burning wood crib received considerable feedback from the ceiling above, somewhat similar to the small crib at the end.

The energy released from the wood crib (i.e., the area under the HRR curve) was 82% of the energy content of the initial mass of the crib. This is a good match with the assumed combustion efficiency of 0.8 and confirms that the measuring method for the mass loss rate and the method to determine the HRR based on this was suitable. The energy released from the CLT (i.e., the area under the HRR-curve) was 97% of the energy of the mass loss, and therefore 17% points higher than what it should have been when using a combustion efficiency of 0.8. The deviation can be explained by some uncertainties in both the method to estimate the total mass loss and the method to determine the HRR from the charring rate. Such a deviation is therefore considered to be acceptable.

The maximum HRR of the CLT was approximately the same as the peak HRR of the wood crib, although lower in general. This is shown by comparing the total energy released from the wood crib and the CLT. 61% of the total energy released originated from the wood crib, and 39% from the CLT.

Besides the own HRR contribution from the CLT, it also increased the HRR of the wood crib. This is clearly shown by comparing the wood crib fire spread rate before and after the ignition of the ceiling. Without the contribution from the CLT, the wood crib fire would have developed much slower, which is indicated by Fig. 8. Here, the flame base area was almost constant between 20 and 33 min before ignition of the ceiling as the leading and trailing edge of the fire travelled at approximately the same rate.

4.5. Char depth and delamination

The char depth was strongly non-uniform across the ceiling, see Fig. 26. The reason for the uneven charring is believed to be caused by temperature and oxygen differences throughout the compartment. The largest char depth along the X-axis was located where the highest temperatures were measured, see Figs. 15 and 19. The lower char dept at the left end of the compartment, where the fire had been present for the longest time, is likely due to the fire in the first 30 min being relatively small with low temperatures below the ceiling. Also, the duration of the post-flashover phase was the shortest at this end. The differences in Y-direction are believed to be due to a higher oxygen concentration under the ceiling in the back of the room compared to the window side. However, this cannot be proven, as the oxygen measurement in the back of the room probably was affected by a leakage.

The arithmetic average of the char depth of the entire CLT ceiling was 26 mm. This is 14 mm from the glue line, and pronounced delamination was unexpected. However, some delamination occurred in the centre of the compartment, see Fig. 27(a), where the char depth was thicker, see Fig. 26. Visual examinations after the experiment showed that even for the areas with delamination, the charring had not reached the glue-line. Hence, delamination must have occurred due to the adhesive losing its bonding properties at lower temperatures than the charring temperature. Precisely at which temperatures delamination occurred cannot be determined. However, the maximum temperature at 40 mm depth was 164–194 °C, around 120 min. It is, therefore, likely that the delamination also occurred around that time. An argument supporting this is the discolouring of the second layer (Fig. 27a), which is known to occur around 200 °C [63,67]. This is close to the measured temperatures at the glue line. In addition, the temperature below the ceiling at 120 min was approx. 220 °C and declining. This low temperature can explain why the charring did not continue into the second layer and caused a reignition.

The main reason for the limited delamination was the combination of a relatively short post-flashover phase and the thick outer layer of 40 mm. A CLT element with a thinner outer layer (e.g., 30 mm) would likely have delaminated on the entire ceiling area in a similar fire.

Nevertheless, this result aligns with a few other experiments [4,21] by showing that delamination of CLT does not always lead to a second flashover. Also worth highlighting is that self-extinguishment of the CLT in this experiment was achieved despite using an adhesive that lacks a demonstrated resistance against glue-line integrity failure.

The char depth is often linked to the duration of the fire or the fuel load density. However, it is essential to note that the heat release rate and the temperature in the compartment also play a role here. This is shown by comparing this experiment to the CodeRed-experiments, where the fuel load density was 50% compared to this experiment (186 vs 353 MJ/m^2). Despite a lower fuel load density and shorter fire duration in the CodeRed experiments, the CLT burnt for about the same time (12 vs 15 min), and the char depths were about the same (25 vs 26 mm). This comparison shows that the total char depth cannot be

determined based on the fuel load density alone. A similar conclusion was made in the Epernon experiments [19].

4.6. External flames

External flames were present during the flashing waves and for a short period after flashover. The external flames were clearly lower from Window 1 than from the other windows, see Fig. 9 (d). This can be explained by the crib being almost completely burnt out in this section of the compartment at flashover. The most intense burning phase and the presence of external flames were short. This is shown through temperatures and heat fluxes in Figs. 21 and 22. Generally, the incident heat flux is lower than the highest values measured in comparable CLT compartment experiments [4,5,9]. This is as expected since most other experiments have been ventilation-controlled, in contrast to the large ventilation openings here, allowing for a larger fraction of the combustible gases to be burnt inside the compartment. In addition, with the large openings, the excess pyrolysis gases were burnt over a larger area, with correspondingly shorter flame height, compared to if the openings had been slimmer [8].

4.7. Ventilation conditions

This experiment had a larger opening factor than the majority of performed CLT experiments, and it would be considered a fuel-controlled fire (Regime-II) based on the traditional distinction for compartment fires [63]. An observation throughout the experiment was the lack of visible smoke during large periods of the fire. This indicates a clean and complete combustion and corresponds well with the relatively high oxygen concentration measured out of Windows 2 and 4. The lack of smoke is also a visual proof of the compartment fire being fuel-controlled during most of the experiment. However, an observation that contradicts the fire to be fuel-controlled was the large external flames at the peak of the 3rd flashing wave and flashover. Their presence shows that a large fraction of the combustible gases produced were burnt on the outside. Such behaviour would typically be considered for ventilation-controlled fires as a sign of too little oxygen to burn the gases inside the compartment. However, as the outflowing gas had an oxygen concentration of minimum 9.5–12%, the non-burned combustible gases were likely a result of insufficient mixing of oxygen and combustible gases.

Summarised, the fire appeared neither as a true fuel-controlled fire nor a ventilation-controlled fire, as it had elements of both. In several ways, this appearance matches the new proposed regime [72], *Regime-II-CLT*. A characteristic of this regime is the higher outflow velocities and less time for sufficient mixing, in which both would lead to a larger external flame. This adapts well to the observations in this experiment. Another characteristic of Regime-II-CLT is that the highest temperatures should be present in the centre height of the room due to insufficient mixing below the ceiling, but this does not match the temperature profile observed in this experiment.

5. Conclusion

A large-scale compartment (95 m^2) fire experiment with an exposed CLT ceiling has been performed. The setup was designed to fill a gap in the current knowledge about fire spread and fire dynamics in large, well-ventilated open-plan compartments with a CLT ceiling. This experiment is among the largest CLT experiments conducted to date and gives a unique perspective on fire dynamics related to an open-plan compartment with an exposed CLT ceiling and large window openings.

- Ignition of the ceiling occurred first at 32.5 min, which could be explained by flames not reaching the ceiling and limited conditions for a thick smoke layer to build up.
- From the point when the ceiling was ignited, the fire dynamics changed completely, and the flames spread quickly across the ceiling and wood crib. Instead of developing into a full flashover directly, the fire travelled back and forth in four distinct flashing waves within 13 min, whereby the wood crib fire grew larger for each wave. Such flashing waves are a new observation for travelling fires.
- The average fire spread rate before the ignition of the ceiling was 54 mm/min (0.9 mm/s), while the rate was 1.2 m/min (20 mm/s) after the ignition of the ceiling. This strengthens previous findings that a CLT ceiling greatly influences the fire spread rate and fire dynamics from the point the ceiling is ignited.
- After a short post-flashover phase, the intensity of the fire was rapidly reduced, and the CLT ceiling self-extinguished over a period of approx. 10 min while the wood crib fire was still burning.
- The charring was most pronounced in the centre of the ceiling and towards the back of the room.
- Some delamination was observed, although the average char depth did not reach the glue line. No reignition or fire growth was observed within 4 h. It is highlighted that this was achieved despite using an adhesive that lacks a demonstrated resistance against glue-line integrity failure.
- External flames were present during the flashing waves and for a short period after flashover. The incident heat flux at the façade was lower than the highest values measured in other comparable CLT compartment experiments.
- The experiment presented here differs significantly from those previously published by having a larger opening factor, the flames did not impinge the ceiling, and there was less potential for combustible gases to accumulate under the ceiling. The rate of fire development was in strong contrast to that of previous experiments and may be relevant for compartment designs with a low likelihood of ceiling-impinging flames (e.g., with a high ceiling) and a low potential for collection of combustible gases under the ceiling, e.g., compartments with ceiling beams of limited height.

Sample CRediT author statement

Andreas Sæter Bøe: Conceptualization, Methodology, Investigation, Formal Analysis, Data Curation, Writing - Original Draft, Writing - Review & Editing, Visualization. Kathinka Leikanger Friquin: Conceptualization, Methodology, Writing - Review & Editing. Daniel Brandon: Conceptualization, Methodology, Writing - Review & Editing. Anne Steen-Hansen: Conceptualization, Writing - Review & Editing. Ivar S. Ertesvåg: Conceptualization, Writing - Review & Editing.

Declaration of competing interest

The authors declare that they have no known competing financial interests or personal relationships that could have appeared to influence the work reported in this paper.

Data availability

Data will be made available on request.

Acknowledgement

The experiments were conducted at RISE Fire Research in Norway as part of the Fire Research and Innovation Centre (FRIC) (www.fric.no). The authors gratefully acknowledge the financial support by the Research Council of Norway through the program BRANNSIKKERHET, project number 294649, and by partners of the research centre FRIC. A special thanks to the FRIC partners StoraEnso, Rockwool, Hunton, and to Saint-Gobain AS and Byggmakker Handel AS for providing building materials. The authors also wish to thank Panos Kotsovinos and David Barber at ARUP, David Lange and Juan P. Hidalgo at The University of

Queensland, and Johan Sjöström at RISE for valuable discussions in the planning phase of the experiments.

Appendix A. Supplementary data

Supplementary data to this article can be found online at https://doi.org/10.1016/j.firesaf.2023.103869.

References

[1] A. Bartlett, A. Law, Influence of excess fuel from timber lined compartments, Construct. Build. Mater. 235 (2020), 117355, https://doi.org/10.1016/j.conbuildmat.2019.117355.

[2] A. Frangi, M. Fontana, Fire performance of timber structures under natural fire conditions, Fire Saf. Sci. 8 (2005) 279–290, https://doi.org/10.3801/IAFSS.FSS.8-279.

[3] T. Hakkarainen, Post-flashover fires in light and heavy timber construction compartments, Post-Flashover Fires Light Heavy Timber Constr. Compart. 20 (2) (2002). https://journals.sagepub.com/doi/abs/10.1177/0734904102020002074.

[4] J. Su, P.-S. Lafrance, M.S. Hoehler, M.F. Bundy, Fire Safety Challenges of Tall Wood Buildings–phase 2: Task 3-Cross Laminated Timber Compartment Fire Tests. Report No. FPRF-2018-01-REV, NFPA (National Fire Protection Association), Quincy, Massachusetts, USA, 2018. Accessed: March 28, 2023. [Online]. Available: https://tsapps.nist.gov/publication/get_pdf.cfm?pub_id=925297.

[5] J. Sjöström, D. Brandon, A. Temple, E. Hallberg, F. Kahl, RISE Report - Exposure from Mass Timber Compartment Fires to Facades (2021:39), RISE Fire Research, 2021.

[6] L.A. Bisby, A. Bartlett, R. McNamee, J. Zehfuss, J.-M. Franssen, F. Robert, C. Tessier, S. Mohaine, Epernon Fire Tests Programme – Synthesis Report, 2020.

[7] R. McNamee, J. Zehfuss, A.I. Bartlett, M. Heidari, F. Robert, L.A. Bisby, Enclosure fire dynamics with a cross-laminated timber ceiling, Fire Mater. 45 (7) (2020) 847–857, https://doi.org/10.1002/fam.2904.

[8] J. Sjöström, D. Brandon, A. Temple, J. Anderson, R. McNamee, External fire plumes from mass timber compartment fires—comparison to test methods for regulatory compliance of façades, Fire Mater. (2023), https://doi.org/10.1002/fam.3129 n/a, no. n/a.

[9] T. Engel, N. Werther, Impact of mass timber compartment fires on façade fire exposure, Fire Technol. 59 (2023) 517–588, https://doi.org/10.1007/s10694-022-01346-8.

[10] R.M. Hadden, A.I. Bartlett, J.P. Hidalgo, S. Santamaria, F. Wiesner, L.A. Bisby, S. Deeny, B. Lane, Effects of exposed cross laminated timber on compartment fire dynamics, Fire Saf. J. 91 (2017) 480–489, https://doi.org/10.1016/j.firesaf.2017.03.074.

[11] X. Li, X. Zhang, G. Hadjisophocleous, C. McGregor, Experimental study of combustible and non-combustible construction in a natural fire, Fire Technol. 51 (6) (2015) 1447–1474, https://doi.org/10.1007/s10694-014-0407-4.

[12] A.R. Medina Hevia, Fire Resistance of Partially Protected Cross-Laminated Timber Rooms, Master thesis, Carleton University, Ottawa, Ontario, 2014.

[13] R. Emberley, T. Do, J. Yim, J.L. Torero, Critical heat flux and mass loss rate for extinction of flaming combustion of timber, Fire Saf. J. 91 (2017) 252–258, https://doi.org/10.1016/j.firesaf.2017.03.008, 2017/07/01.

[14] R. Crielaard, J.-W. van de Kuilen, K. Terwel, G. Ravenshorst, P. Steenbakkers, Self-extinguishment of cross-laminated timber, Fire Saf. J. 105 (2019) 244–260, https://doi.org/10.1016/j.firesaf.2019.01.008, 2019/04/01.

[15] T. Ohlemiller, Smoldering Combustion. SFPE Handbook of Fire Protection Engineering, Society of Fire Protection Engineers, 2002.

[16] J. Cuevas, J.L. Torero, C. Maluk, Flame extinction and burning behaviour of timber under varied oxygen concentrations, Fire Saf. J. 120 (2021), 103087, https://doi.org/10.1016/j.firesaf.2020.103087, 2021/03/01.

[17] P. Kotsovinos, E. Rackauskaite, E. Christensen, A. Glew, E. O'Loughlin, H. Mitchell, R. Amin, F. Robert, M. Heidari, D. Barber, G. Rein, J. Schulz, Fire dynamics inside a large and open-plan compartment with exposed timber ceiling and columns: CodeRed #01, Fire Mater. (2022), https://doi.org/10.1002/fam.3049 vol. n/a, no. n/a.

[18] D. Brandon, J. Sjöström, A. Temple, E. Hallberg, F. Kahl, RISE Report - Final Project Report - Fire Safe Implementation of Visible Mass Timber in Tall Buildings - Compartment Fire Testing (2021:40), RISE Fire Research, 2021 [Online]. Available: http://urn.kb.se/resolve?urn=urn:nbn:se:ri:diva-58153.

[19] F. Wiesner, A. Bartlett, S. Mohaine, F. Robert, R. McNamee, J.-C. Mindeguia, L. Bisby, Structural capacity of one-way spanning large-scale cross-laminated timber slabs in standard and natural fires, Fire Technol. 57 (1) (2021) 291–311, https://doi.org/10.1007/s10694-020-01003-y, 2021/01/01.

[20] T. Gernay, J. Zehfuß, S. Brunkhorst, F. Robert, P. Bamonte, R. McNamee, S. Mohaine, J.-M. Franssen, Experimental investigation of structural failure during the cooling phase of a fire: timber columns, Fire Mater. 47 (4) (2023) 445–460, https://doi.org/10.1002/fam.3110.

[21] D. Hopkin, W. Węgrzyński, M. Spearpoint, I. Fu, H. Krenn, T. Sleik, C. Gorska, G. Stapf, Large-scale enclosure fire experiments adopting CLT slabs with different types of polyurethane adhesives: genesis and preliminary findings, Fire 5 (2) (2022), https://doi.org/10.3390/fire5020039.

[22] R. Emberley, C.G. Putynska, A. Bolanos, A. Lucherini, A. Solarte, D. Soriguer, M. G. Gonzalez, K. Humphreys, J.P. Hidalgo, C. Maluk, A. Law, J.L. Torero, Description of small and large-scale cross laminated timber fire tests, Fire Saf. J. 91 (2017) 327–335, https://doi.org/10.1016/j.firesaf.2017.03.024, 2017/07/01.

[23] C. Gorska, PhD Thesis - Fire Dynamics in Multi Scale Timber Compartments, PhD, The University of Queensland, Australia, 2019.

[24] M. Hoehler, J. Su, P.-S. Lafrance, M. Bundy, A. Kimball, D. Brandon, B. Östman, Fire safety challenges of tall wood buildings : large-scale cross-laminated timber compartment fire tests, in: Presented at the SiF 2018 - the 10th International Conference on Structures in Fire, 2018. Belfast, UK, 2018. [Online]. Available: http://urn.kb.se/resolve?urn=urn:nbn:se:lnu:diva-77612.

[25] J. Liu, E.C. Fischer, Review of large-scale CLT compartment fire tests, Constr. Build. Mater. 318 (2022), 126099, https://doi.org/10.1016/j.conbuildmat.2021.126099.

[26] G. Ronquillo, D. Hopkin, M. Spearpoint, Review of large-scale fire tests on cross-laminated timber, J. Fire Sci. 39 (5) (2021) 327–369, https://doi.org/10.1177/07349041211034460.

[27] J.L. Torero, A.H. Majdalani, C. Abecassis-Empis, A. Cowlard, Revisiting the compartment fire, Fire Saf. Sci. 11 (2014) 28–45.

[28] V. Gupta, J.P. Hidalgo, D. Lange, A. Cowlard, C. Abecassis-Empis, J.L. Torero, A review and analysis of the thermal exposure in large compartment fire experiments, Int. J. High-Rise Build.g 10 (4) (2021) 345–364, https://doi.org/10.21022/IJHRB.2021.10.4.345.

[29] J.P. Hidalgo, A. Cowlard, C. Abecassis-Empis, C. Maluk, A.H. Majdalani, S. Kahrmann, R. Hilditch, M. Krajcovic, J.L. Torero, An experimental study of full-scale open floor plan enclosure fires, Fire Saf. J. 89 (2017) 22–40, https://doi.org/10.1016/j.firesaf.2017.02.002.

[30] A. Nadjai, A. Naveed, M. Charlier, O. Vassart, S. Welsh, A. Glorieux, J. Sjostrom, Large scale fire test: the development of a travelling fire in open ventilation conditions and its influence on the surrounding steel structure, Fire Saf. J. 130 (2022), 103575, https://doi.org/10.1016/j.firesaf.2022.103575, 2022/06/01.

[31] E. Rackauskaite, M. Bonner, F. Restuccia, N. Fernandez Anez, E.G. Christensen, N. Roenner, W. Wegrzynski, P. Turkowski, P. Tofilo, M. Heidari, P. Kotsovinos, I. Vermesi, F. Richter, Y. Hu, C. Jeanneret, R. Wadhwani, G. Rein, Fire experiment inside a very large and open-plan compartment: x-ONE, Fire Technol. 58 (2022) 905–939, https://doi.org/10.1007/s10694-021-01162-6.

[32] M. Heidari, E. Rackauskaite, M. Bonner, E. Christensen, S. Morat, H. Mitchell, P. Kotsovinos, P. Turkowski, W. Wegrzynski, P. Tofilo, G. Rein, Fire experiments inside a very large and open-plan compartment: x-TWO, in: Presented at the Proceedings of the 11th International Conference on Structures in Fire (SiF2020), The University of Queensland, Brisbane, Australia, 2020.

[33] D. Rush, X. Dai, D. Lange, Tisova fire test – fire behaviours and lessons learnt, Fire Saf. J. 121 (2021), 103261, https://doi.org/10.1016/j.firesaf.2020.103261, 2021/05/01.

[34] S. Nothard, D. Lange, J.P. Hidalgo, V. Gupta, M.S. McLaggan, F. Wiesner, J. L. Torero, Factors influencing the fire dynamics in open-plan compartments with an exposed timber ceiling, Fire Saf. J. 129 (2022), 103564, https://doi.org/10.1016/j.firesaf.2022.103564, 2022/05/01.

[35] J.P. Hidalgo, T. Goode, V. Gupta, A. Cowlard, C. Abecassis-Empis, J. Maclean, A. I. Bartlett, C. Maluk, J.M. Montalvá, A.F. Osorio, J.L. Torero, The Malveira fire test: full-scale demonstration of fire modes in open-plan compartments, Fire Saf. J. 108 (2019), https://doi.org/10.1016/j.firesaf.2019.102827.

[36] P. Kotsovinos, E.G. Christensen, E. Rackauskaite, A. Glew, E. O'Loughlin, H. Mitchell, R. Amin, F. Robert, M. Heidari, D. Barber, G. Rein, J. Schulz, Impact of ventilation on the fire dynamics of an open-plan compartment with exposed timber ceiling and columns: CodeRed #02, Fire Mater. (2022), https://doi.org/10.1002/fam.3082.

[37] H.E. Nelson, Engineering View of the Fire of May 4, 1988 in the First Interstate Bank Building, 1989. Los Angeles, California (NIST IR 89-4061).

[38] B.R. Kirby, D.E. Wainman, L.N. Tomlinson, T.R. Kay, B.N. Peacock, Natural fires in large scale compartments, Int. J. Eng. Perf.-Bases Fire Codes 1 (2) (1999) 43–58.

[39] R.G. Gann, A. Hamins, K. McGrattan, H.E. Nelson, T.J. Ohlemiller, K.R. Prasad, W. M. Pitts, Reconstruction of the fires and thermal environment in World Trade Center buildings 1, 2, and 7, Fire Technol. 49 (2013) 679–707.

[40] J. Gales, Travelling fires and the st. Lawrence burns project, Fire Technol. 50 (2014) 1535–1543, https://doi.org/10.1007/s10694-013-0372-3.

[41] J.G. Quintiere, Principles of Fire Behavior, second ed., CRC Press, 2016.

[42] NFPA 1710, Standard for the Organization and Deployment of Fire Suppression Operations, Emergency Medical Operations, and Special Operations to the Public by Career Fire Departments, 2020. Quincy, MA.

[43] E. Rackauskaite, P. Kotsovinos, D. Barber, Letter to the editor: design fires for open-plan buildings with exposed mass-timber ceiling, Fire Technol. 57 (2) (2021) 487–495, https://doi.org/10.1007/s10694-020-01047-0, 2021/03/01.

[44] H. Mitchell, P. Kotsovinos, F. Richter, D. Thomson, D. Barber, G. Rein, Review of fire experiments in mass timber compartments: current understanding, limitations, and research gaps, Fire Mater. (2022), https://doi.org/10.1002/fam.3121 vol. n/a, no. n/a.

[45] EN 1991 1-2 (2002), Eurocode 1: Actions on Structures – Part 1-2: General Actions - Actions on Structures Exposed to Fire, CEN, Brussels, Belgium, 2002.

[46] EAD 130005-00-0304, Solid Wood Slab Element to Be Used as a Structural Element in Buildings, EOTA, Brussels, Belgium, 2015.

[47] EN 520:2004+A1:2009, Gypsum Plasterboards - Definitions, Requirements and Test Methods, CEN, Brussels, Belgium, 2004.

[48] ISO 12570:2000, Hygrothermal Performance of Building Materials and Products-Determination of Moisture Content by Drying at Elevated Temperature, ISO, Brussels, Belgium, 2000, 2000.

[49] V. Gupta, J.L. Torero, J.P. Hidalgo, Burning dynamics and in-depth flame spread of wood cribs in large compartment fires, Combust. Flame 228 (2021) 42–56, https://doi.org/10.1016/j.combustflame.2021.01.031.

[50] IEC 60584-1:2013, Thermocouples - Part 1: EMF Specifications and Tolerances, IEC, Brussels, Belgium, 2013.
[51] EN 1363-1:2020, Fire Resistance Tests - Part 1: General Requirements, CEN, Brussels, Belgium, 2020.
[52] U. Wickström, Temperature Calculation in Fire Safety Engineering, Springer, 2016.
[53] EN 1991-1-2 (2002), CEN, Brussels, Belgium, 2002.
[54] M.S. Hoehler, On the development of a transparent enclosure for 360° video cameras to observe severe fires in situ, Fire Saf. J. 120 (2021/03/01/2021), 103024, https://doi.org/10.1016/j.firesaf.2020.103024.
[55] ISO 9705-1, Reaction to Fire Tests - Room Corner Test for Wall and Ceiling Lining Products - Part 1: Test Method for a Small Room Configuration, ISO, Switzerland, 2016.
[56] I. Pope, J.P. Hidalgo, R.M. Hadden, J.L. Torero, A simplified correction method for thermocouple disturbance errors in solids, Int. J. Therm. Sci. 172 (2022), 107324, https://doi.org/10.1016/j.ijthermalsci.2021.107324, 2022/02/01.
[57] R. Fahrni, J. Schmid, M. Klippel, A. Frangi, Correct temperature measurements in fire exposed wood, in: Presented at the World Conference on Timber Engineering (WCTE), Seoul, South Korea, 2018.
[58] J.V. Beck, Thermocouple temperature disturbances in low conductivity materials, J. Heat Tran. 84 (2) (1962) 124–131, https://doi.org/10.1115/1.3684310.
[59] EN 1995-1-2 (Eurocode 5), Design of Timber Structures – Part 1-2: General - Structural Fire Design, CEN, Brussels, Belgium, 2004.
[60] J. Schmid, M. Klippel, M. Viertel, R. Presl, R. Fahrni, A. Totaro, A. Frangi, Charring of timber - determination of the residual virgin cross-section and charring rates, in: Presented at the World Conference on Timber Engineering 2020, Santiago, Chile, 2020.
[61] M. Aniszewska, A. Gendek, Comparison of heat of combustion and calorific value of the cones and wood of selected forest trees species, For. Res. Pap. 75 (3) (2014) 231–236 [Online]. Available: https://depot.ceon.pl/handle/123456789/5332.
[62] B.J. McCaffrey, G. Heskestad, A robust bidirectional low-velocity probe for flame and fire application, Combust. Flame 26 (1976) 125–127, https://doi.org/10.1016/0010-2180(76)90062-6, 1976/02/01.
[63] D. Drysdale, An Introduction to Fire Dynamics, third ed., John Wiley & sons, 2011.
[64] Z. Nan, A.A. Khan, L. Jiang, S. Chen, A. Usmani, Application of travelling behaviour models for thermal responses in large compartment fires, Fire Saf. J. 134 (2022), 103702, https://doi.org/10.1016/j.firesaf.2022.103702, 2022/12/01.
[65] J.G. Quintiere, A.S. Rangwala, A theory for flame extinction based on flame temperature, Fire Mater. 28 (5) (2004) 387–402, https://doi.org/10.1002/fam.835.
[66] H. Xu, I. Pope, V. Gupta, J. Cadena, J. Carrascal, D. Lange, M.S. McLaggan, J. Mendez, A. Osorio, A. Solarte, D. Soriguer, J.L. Torero, F. Wiesner, A. Zaben, J. P. Hidalgo, Large-scale compartment fires to develop a self-extinction design framework for mass timber—Part 1: literature review and methodology, Fire Saf. J. 128 (2022), 103523, https://doi.org/10.1016/j.firesaf.2022.103523, 2022/03/01.
[67] A.I. Bartlett, R.M. Hadden, L.A. Bisby, A review of factors affecting the burning behaviour of wood for application to tall timber construction, Fire Technol. 55 (1) (2019) 1–49, https://doi.org/10.1007/s10694-018-0787-y, 2019/01/01.
[68] A. Law, R. Hadden, We need to talk about timber: fire safety design in tall buildings, Struct. Eng. (3) (2020).
[69] D. Brandon, B. Östman, Fire Safety Challenges of Tall Wood Buildings – Phase 2: Task 1 - Literature Review, NFPA, 2016.
[70] F. Richter, F.X. Jervis, X. Huang, G. Rein, Effect of oxygen on the burning rate of wood, Combust. Flame 234 (2021), 111591, https://doi.org/10.1016/j.combustflame.2021.111591, 2021/12/01.
[71] D.C.O. Marney, L.J. Russell, R. Mann, Fire performance of wood (Pinus radiata) treated with fire retardants and a wood preservative, Fire Mater. 32 (6) (2008) 357–370, https://doi.org/10.1002/fam.973, 2008/10/01.
[72] C. Gorska, J.P. Hidalgo, J.L. Torero, Fire dynamics in mass timber compartments, Fire Saf. J. 120 (2021), https://doi.org/10.1016/j.firesaf.2020.103098.